Synthesis of a Series of Diiron Complexes Based on a Tetraethynylethene Skeleton and Related C_6-Enediyne Spacers, (dppe)Cp*Fe−C≡CC(R)═C(R)C≡C−FeCp*(dppe): Tunable Molecular Wires§

Munetaka Akita,*,† Yuya Tanaka,† Chie Naitoh,† Takehiro Ozawa,† Nobuhiko Hayashi,† Makoto Takeshita,† Akiko Inagaki,† and Min-Chul Chung‡

Chemical Resources Laboratory, Tokyo Institute of Technology, R1-27, 4259 Nagatsuta, Midori-ku, Yokohama 226-8503, Japan, and Department of Chemical Engineering, Sunchon National University, 315 Maegok-dong, Sunchon, Jeonnam 540-742, Republic of Korea

Received May 11, 2006

A series of 3,4-disubstituted (hex-3-ene-1,5-diyne-1,6-diyl)diiron complexes with FeCp*(dppe) (***Fe***) end caps, ***Fe***−C≡CC(R)═C(R)C≡C−***Fe*** (R = H, C≡C−$SiMe_3$, C≡C−H, C_6H_5, *p*-$C_6H_4CF_3$), and the related (octa-3,5-diene-1,7-diyne-1,8-diyl)diiron complex, ***Fe***−C≡C−C(H)═C(H)C(H)═C(H)C≡C−***Fe***, has been prepared, and their performance as molecular wires has been evaluated. The enyne complexes have been synthesized via vinylidene intermediates, [***Fe***═C═C(H)C(R)═C(R)C(H)═C═***Fe***]$^{2+}$, derived from the corresponding terminal alkynes or the Me_3Si-protected precursors (XC≡CCC(R)═C(R)C≡C−X; X = H, $SiMe_3$), and the products have been characterized spectroscopically and crystallographically. The performance of the obtained dinuclear enyne complexes as molecular wires has been evaluated on the basis of the comproportionation constants (K_C) obtained by electrochemical measurements and the V_{ab} values obtained from the spectral parameters of the intervalence charge transfer bands of the isolated monocationic radical species appearing in the near-IR region. As a result, the C_6-enediyne complexes turn out to be excellent molecular wires, with K_C values larger than 10^8 as well as V_{ab} values larger than 0.35, belonging to class III compounds according to the Robin and Day classification and being comparable to the related polyynediyl complexes as well. It is notable that, in the enyne system, the performance can be readily tuned by introduction of appropriate substituents onto the olefinic part. Thus, diiron complexes containing an enyne spacer can be regarded as tunable molecular wires.

Introduction

Dinuclear metal complexes connected by a linear π-conjugated bridging ligand have attracted increasing attention because of their potential utility as molecular wires, which are indispensable components for molecular electronics.[1,2] In particular, those with redox-active metal termini have been most extensively studied. The electron-donating metal end caps can stabilize the radical species resulting from oxidation, and their performance as wires is conveniently evaluated in terms of their electrochemical properties.[3] Of the variety of structural motifs of the linker studied so far, polyynediyl bridges ($(C{\equiv}C)_n$ (**A**^{n}); Scheme 1) have proven to be excellent, as revealed by the extensive studies by Lapinte on the FeCp*(diphosphine) complexes (Cp* = η^5-C_5Me_5)[4] and by other researchers on other metal complexes.[5−7] On the other hand, we have studied **A**^{n}-type polyynediyldiiron complexes, Fp*−$(C{\equiv}C)_n$−Fp* (Fp* = $FeCp^*(CO)_2$), from a different point of view, and we revealed that a series of this type of compound with up to six C≡C units (C_{12}) provided versatile precursors for polycarbon cluster compounds.[8] Taking into consideration these situations, we turned our attention to higher order systems, i.e., two- and three-dimensional communication systems, where diversity in the structural motifs and the direction of the intermetallic communication are enriched.

Scheme 1

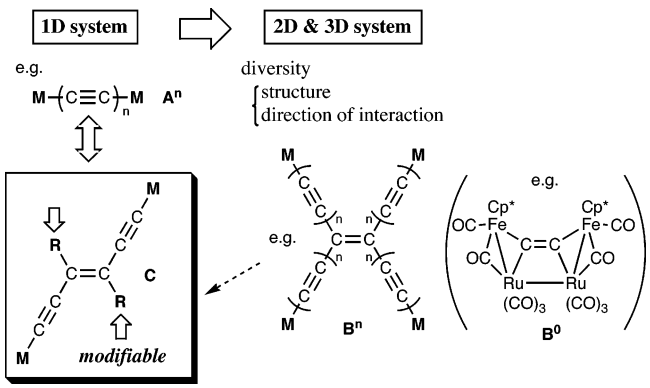

§ This paper is dedicated to Professor John R. Shapley on the occasion of his 60th birthday, in recognition of his outstanding contributions to organometallic chemistry.

* To whom correspondence should be addressed. E-mail: makita@res.titech.ac.jp.

† Tokyo Institute of Technology.

‡ Sunchon National University.

(1) Jortner, J.; Ratner, M. A. *Molecular Electronics*; Blackwell Science: Oxford, U.K., 1997. Aviram, A.; Ratner, M. *Ann. N.Y. Acad. Sci.* **1998**, 852. Ratner, M. *Nature* **2000**, *404*, 137. Tour, J. M. *Acc. Chem. Res.* **2000**, *33*, 791. Hipps, K. W. *Science* **2001**, *284*, 536. Cahen, D.; Hodes, G. *Adv. Mater.* **2002**, *14*, 789. Caroll, R. L.; Gorman, C. B. *Angew. Chem., Int. Ed.* **2002**, *41*, 4378. Robertson, N.; McGowan, G. A. *Chem. Soc. Rev.* **2003**, *32*, 96. *Molecular Nanoelectronics*; Reed, M. A., Lee, T., Eds.; American Scientific: Stevenson Ranch, CA, 2003. Flood, A. H.; Stoddart, J. F.; Steuerman, D. W.; Heath, J. R. *Science* **2004**, *306*, 2055. Nørgaard, K.; Bjørnholm, T. *Chem. Commun.* **2005**, 1812. Benniston, A. C. *Chem. Soc. Rev.* **2004**, *33*, 573. Low, P. J. *Dalton Trans.* **2005**, 2821.

(2) (a) Schwab, P. F. H.; Levin, M. D.; Michl, J. *Chem. Rev.* **1999**, *99*, 1863. (b) Schwab, P. F. H.; Smith, J. R.; Michl, J. *Chem. Rev.* **2005**, *105*, 1197.

(3) Bruce, M. I.; Low, P. J. *Adv. Organomet. Chem.* **2004**, *50*, 231.

10.1021/om060403t CCC: $33.50
Publication on Web 09/23/2006

Typical structural motifs for the core part of the two-dimensional (2D) systems involve olefin and benzene frameworks. Although their permetalated derivatives ($M_2C{=}CM_2$ and C_6M_6) would be suitable for the study of intermetallic communication, very few examples of such derivatives have been reported so far. Previously we reported permetalated ethene derivatives (**B**^{0}; Scheme 1)[8c,d,9] but the metal centers are connected by additional metal−metal bonds, through which the metal centers can also communicate. The lack of permetalated derivatives without metal−metal bonds can be attributed to the bulky metal fragment, which prevents multiple metalation of the central carbon core. This disadvantageous point could be overcome through insertion of a π-conjugated linker (e.g., acetylene unit) as shown in Scheme 1 to separate the metal centers, as typically exemplified for the ethene derivatives (**B**^{n} ($n > 0$)). The organic systems of the core parts of **B**^{n} (e.g. $n =$ 1: tetraethynylethene (TEE)) and the benzene counterparts have been studied extensively by Diederich[10] and Vollhardt,[11] respectively, and their chemical properties and extension to higher systems have also been their research subjects. However, very few studies on their metal complexes have been reported so far.[12]

Scheme 2

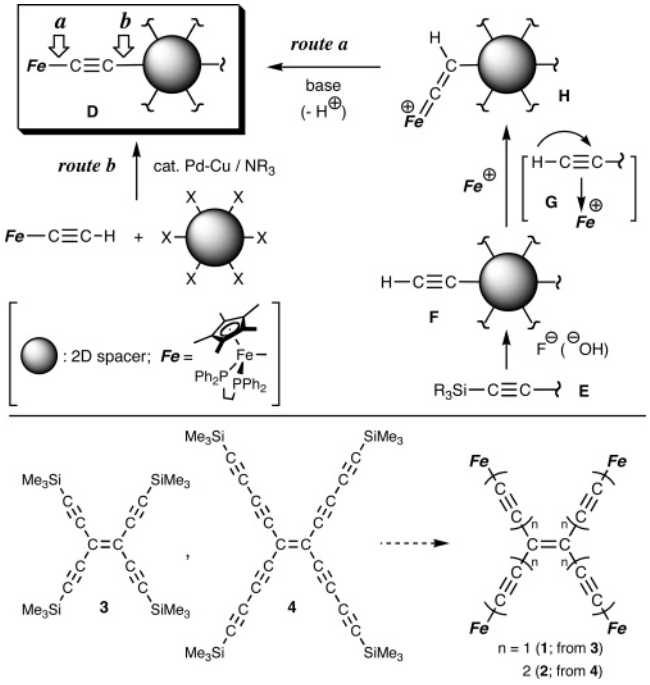

Herein we disclose results of our attempts at the preparation of **B**^{1} and **B**^{2} type olefinic complexes bearing the FeCp*(dppe) fragments (abbreviated as ***Fe*** throughout this paper). Although the attempted preparation of 2D complexes has been unsuccessful, we instead obtained a series of (hex-3-ene-1,5-diyne-1,6-diyl)diiron complexes **C**. In comparison to the related **A**^{3}-type system consisting only of C≡C units, which cannot be functionalized, the properties of the **C**-type complexes can be modified or tuned by introducing appropriate substituents (R) onto the olefinic part, as verified by the present study.

Results and Discussion

Synthesis of Diiron Complexes with π-Conjugated Spacers. (i) Feasible Synthetic Routes to Two-Dimensional (2D) Systems. In principle, two routes (a and b) are feasible for the construction of two-dimensional (2D) systems with FeCp*(dppe) fragments (**D**), and the routes involve Fe−C≡ or ≡C−C(sp^2) bond formation at the last stage (Scheme 2; the routes are exemplified for a poly(ethynyl) derivative). Route a involves deprotonation of the cationic vinylidene intermediate **H**, which can be generated by interaction of the labile solvated cationic

(4) (a) Paul, F.; Lapinte, C. *Coord. Chem. Rev.* **1998**, *178*, 431. (b) Le Narvor, N.; Toupet, L.; Lapinte, C. *Chem. Commun.* **1993**, 357. (c) Le Narvor, N.; Toupet, L.; Lapinte, C. *J. Am. Chem. Soc.* **1995**, *117*, 7129. (d) Le Narvor, N.; Lapinte, C. *C. R. Acad. Sci., Ser. IIc: Chim.* **1998**, *1*, 745. (e) Guillemot, M. Toupet, L.; Lapinte, C. *Organometallics* **1998**, *17*, 1928. (f) Coat, F.; Guillevic, M. A.; Toupet, L.; Paul, F.; Lapinte, C. *Organometallics* **1997**, *16*, 5988. (g) Paul, F.; Meyer, W. E.; Toupet, L.; Jiao, H. J.; Gladysz, J. A.; Lapinte, C. *J. Am. Chem. Soc.* **2000**, *122*, 9405. (h) Jiao, H. J.; Costuas, K.; Gladysz, J. A. Halet, J.-F.; Guillemot, M.; Paul, F.; Lapinte, C. *J. Am. Chem. Soc.* **2003**, *125*, 9511. (i) Bruce, M. I.; Ellis, B. G.; Gaudio, M.; Lapinte, C.; Melino, G.; Paul, F.; Skelton, B. W.; Smith, M. E.; Toupet, L.; White, A. H. *Dalton Trans.* **2004**, 1601. (j) Bruce, M. I.; Costuas, K.; Davin, T.; Ellis, B. G.; Halet, J.-F.; Lapinte, C.; Low, P. J.; Smith, M. E.; Skelton, B. W.; Toupet, L.; White, A. H. *Organometallics* **2005**, *24*, 3864. (k) Coat, F.; Lapinte, C. *Organometallics* **1996**, *15*, 477. (l) Coat, F.; Paul, F.; Lapinte, C.; Toupet, L.; Costuas, K.; Halet, J.-F. *J. Organomet. Chem.* **2003**, *683*, 368. (m) Le Narvor, N.; Lapinte, C. *Organometallics* **1995**, *14*, 634. (n) Weyland, T.; Lapinte, C.; Frapper, G.; Calhorda, M. J.; Halet, J. F.; Toupet, L. *Organometallics* **1997**, *16*, 2024. (o) Weyland, T.; Costuas, K.; Mari, A.; Halet, J. F.; Lapinte, C. *Organometallics* **1998**, *17*, 5569. (p) Weyland, T.; Costuas, K.; Toupet, L.; Halet, J. F.; Lapinte, C. *Organometallics* **2000**, *19*, 4228. (q) de Montigny, F.; Argouarch, G. Costuas, K.; Halet, J. F.; Roisnel, T.; Toupet, L.; Lapinte, C. *Organometallics* **2005**, *24*, 4558. (r) Ibn, G. S.; Paul, F.; Toupet, L. *J. Am. Chem. Soc.* **2006**, *128*, 2463. (s) Le Stang, S.; Paul, F.; Lapinte, C. *Organometallics* **2000**, *19*, 1035. (t) Roue, S.; Lapinte, C.; Bataille, T. *Organometallics* **2004**, *23*, 2558. (u) Bruce, M. I.; de Montigny, F.; Jevric, M.; Lapinte, C.; Skelton, B. W.; Smith, M. E.; White, A. H. *J. Organomet. Chem.* **2004**, *689*, 2860. (v) Bruce. M. I.; Low, P. J.; Hartl, F.; Humphrey, P. A.; de Montigny, F.; Jevric, M.; Lapinte, C.; Perkins, G. J.; Roberts, R. L.; Skelton, B. W.; White, A. H. *Organometallics* **2005**, *24*. 5241. (w) Guillaume, V.; Mahias, V.; Mari, A.; Lapinte, C. *Organometallics* **2000**, *19*, 1422. (x) Le Stang, S.; Paul, F.; Lapinte, C. *Inorg. Chim. Acta* **1999**, *291*, 403. (y) Le Stang, S.; Lenz, D.; Paul, F.; Lapinte, C. *J. Organomet. Chem.* **1999**, *572*, 189. (z) Denis, R., Weyland, T., Paul, F.; Lapinte, C. *J. Organomet. Chem.* **1997**, *546*, 615.

(5) (a) Bruce, M. I.; Low, P. J.; Costuas, K.; Halet, J.-F.; Best, S. P.; Heath, G. A. *J. Am. Chem. Soc.* **2000**, *122*, 1949. (b) Bruce, M. I.; Kelly, B. D.; Skelton, B. W.; White, A. H. *J. Organomet. Chem.* **2000**, *604*, 150. (c) Bruce, M. I.; Ellis, B. G.; Low, P. J.; Skelton, B. W.; White, A. H. *Organometallics* **2003**, *22*, 3184. (d) Bruce, M. I.; Smith, M. E.; Skelton, B. W.; White, A. H. *J. Organomet. Chem.* **2001**, *637-639*, 484.

(6) (a) Brady, M.; Weng, W.; Zhou, Y.; Seyler, J. W.; Amoroso, A. J.; Arif, A. M.; Bohme, M.; Frenking, G.; Gladysz, J. A. *J. Am. Chem. Soc.* **1997**, *119*, 775. (b) Bartik, T.; Weng, W.; Ramsden, J. A.; Szafewrt, S.; Falloon, S. B.; Arif, A. M.; Gladysz, J. A. *J. Am. Chem. Soc.* **1998**, *120*, 11071. (c) Dembinski, R.; Bartik, T.; Bartik, B.; Jaeger, M.; Gladysz, J. A. *J. Am. Chem. Soc.* **2000**, *122*, 810. (d) Zheng, Q.; Gladysz, J. A. *J. Am. Chem. Soc.* **2005**, *127*, 10508.

(7) (a) Touchard, D.; Dixneuf, P. H. *Coord. Chem. Rev.* **1998**, *178−180*, 409. (b) Fernandez, F. J.; Venkatesan, K.; Blacque, O.; Alfonso, M.; Schmalle, H. W.; Berke, H. *Chem. Eur. J.* **2003**, *9*, 6192. (c) Ren, T. *Organometallics* **2005**, *24*, 4854.

(8) (a) Akita, M.; Moro-oka, Y. *Bull. Chem. Soc. Jpn.* **1995**, *68*, 420. (b) Akita, M.; Sakurai, A.; Chung, M.-C.; Moro-oka, Y. *J. Organomet. Chem.* **2003**, *670*, 2. (c) Akita, M.; Sugimoto, S.; Tanaka, M.; Moro-oka, Y. *J. Am. Chem. Soc.* **1992**, *114*, 7581. (d) Akita, M.; Sugimoto, S.; Hirakawa, H.; Kato, S.; Terada, M.; Tanaka, M.; Moro-oka, Y. *Oganometallics* **2001**, *20*, 1555.

(9) Byrne, L. T.; Hos, J. P.; Koutsantonis, G. A.; Skelton, B. W.; White, A. H. *J. Organomet. Chem.* **2000**, *598*, 28.

(10) See, for example: Tykwinski, R. R.; Diederich, F. *Liebigs Ann./Recl.* **1997**, 649. Diederich, F. *Chem. Commun.* **2001**, 219. Diederich, F. *Chem. Rec.* **2002**, *2*, 189.

(11) Diercks, R.; Armstrong, J. C.; Boese, R.; Vollhardt, K. P. C. *Angew. Chem., Int. Ed. Engl.* **1986**, *25*, 270. Boese, R.; Green, J. R.; Mittendorf, J.; Mohler, D. L.; Vollhardt, K. P. C. *Angew. Chem., Int. Ed. Engl.* **1992**, *31*, 1643.

(12) As for the TEE system, Che reported synthesis and luminescence properties of the Au complexes, $C_2(C{\equiv}C{-}Au(PR_3))_4$ and Low[14c] reported μ-η^2:η^2-Co_2 adducts: Lu, W.; Zhu, N.; Che, C. M. *J. Organomet. Chem.* **2003**, *670*, 11. For TEE−Pt_2 complexes, see: Siemsen, P.; Gubler, U.; Bosshard, C.; Günter, P. Diederich, F. *Chem. Eur. J.* **2001**, *7*, 1333. Recently Bruce et al. reported the TEE complexes with the (μ_3-C)$Co_3(CO)_9$ cluster units. Bruce, M. I.; Zaitseva, N. A.; Low, P. J.; Skeleton, B. W.; White, A. H. *J. Organomet. Chem.* **2006**, *691*, 4273.

Scheme 3

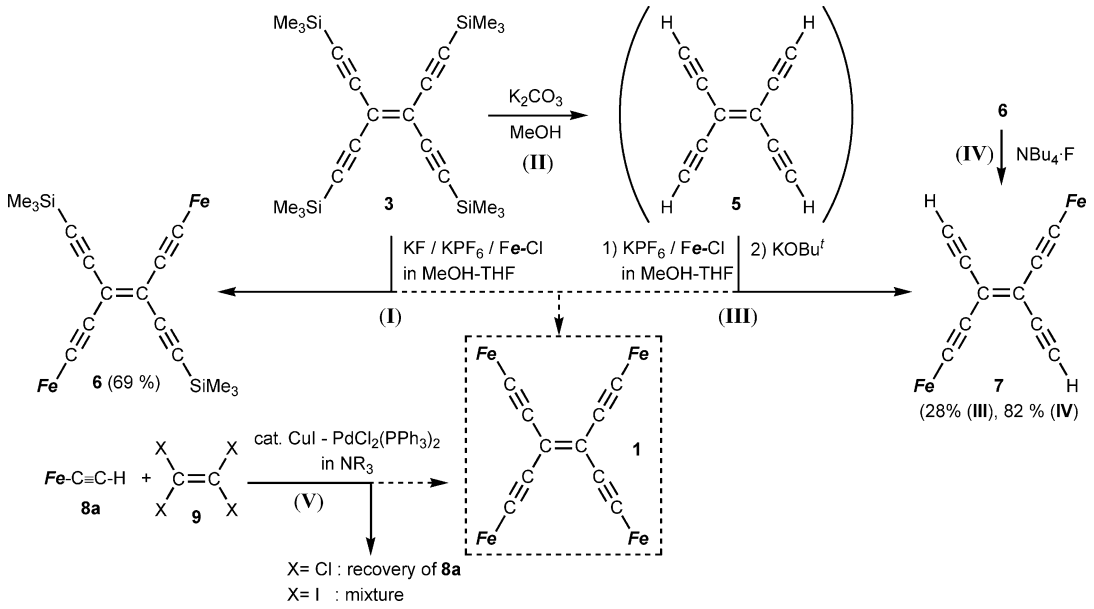

iron species $[FeCp^*(dppe)(solvent)]^+$ with an appropriate polyethynylated compound **F** (via a 1,2-H shift on **G**), as already established by Lapinte.[13] The use of a potentially explosive polyethynylated compound **F** such as tetraethynylethene (TEE; $(HC{\equiv}C)_2C{=}C(C{\equiv}CH)_2$)[14a,b] can be avoided by in situ generation from the corresponding SiR_3-protected precursor **E**. The TEE (**1**) and tetrakis(butadiynyl)ethene complexes (**2**) may be obtained from the corresponding silyl derivatives **3** and **4**, which were reported by Diederich[14] and by us,[15] respectively. The other access (route b) involves multiple Sonogashira coupling between perhalo compounds and the polyynyl complex mediated by the Pd−Cu catalyst system in amine solvent.[16]

(ii) Synthesis of Dinuclear Tetraethynylethene (TEE) Complexes 6 and 7: Attempts at Synthesis of Tetranuclear TEE (1) and Tetrakis(butadiynyl)ethene Derivatives (2). We first examined reactions based on route a. A 1:4 mixture of tetrakis(trimethylsilylethynyl)ethene (**3**)[14] and ***Fe***−Cl dissolved in MeOH-THF was refluxed for 8 h in the presence of KF and KPF_6 (reaction I in Scheme 3),[4,13] and subsequent extraction with ether gave the purple product **6**,[17] which was characterized as the ((*E*)-3,4-bis((trimethylsilyl)ethynyl)hex-3-ene-1,5-diyn-1,6-diyl)diiron complex as described below. It is apparent that the dinuclear TEE complex **6** resulted from partial metalation of the tetrasilyl precursor **3** instead of the desired tetrasubstitution leading to **1**.

Because the incomplete metalation could be attributed to the bulky substituents (***Fe*** and $SiMe_3$), as can be seen from its molecular structure (see below), **3** was desilylated prior to the metalation (reaction II). The desilylation of **3** was readily effected by treatment with a methanolic K_2CO_3 solution according to the procedure reported by Diederich.[14b] (*Caution! Because concentrated **5** is explosive, its solution must not be dried.*) The in situ generated **5** was subjected to reaction with ***Fe***−Cl/KPF_6 in MeOH−THF (reaction III). The low solubility of the reaction product in less polar solvents (e.g. ether and toluene) suggested formation of an **H**-type cationic vinylidene intermediate (Scheme 2), which was subsequently treated with KOBu^t to cause deprotonation. The red-purple product **7**[17] thus obtained was characterized as another dinuclear TEE complex, ((*E*)-3,4-diethynylhex-3-en-1,5-diyne-1,6-diyl)diron complex, resulting from partial metalation, as described below. Again, we could not obtain any evidence for the desired tri- and tetrametalation. The ethynyl derivative **7** was also obtained by desilylation of the Si-protected complex **6** (reaction IV).

Sonogashira coupling (route b; V) between the ethynyl complex **8a**[4c] and tetrahaloethene **9** in NEt_3 resulted in recovery of **8a** (X = Cl) or a complicated mixture of products (X = I).

The failure in preparation of **1** apparently resulting from the steric repulsion caused by the bulky ***Fe*** groups prompted us to examine the butadiynyl derivative **2** with longer C≡C−C≡C linkers, which separate the metal centers at a distance longer than 10 Å.[15] However, metalation of **4** with ***Fe***−Cl (route a in Scheme 2) afforded a complicated mixture of products, and liberation of free dppe ligand suggested the occurrence of decomposition. The Pd−Cu-catalyzed reaction of the butadiynyl complex Fe−C≡C−C≡CH (**8b**)[4f] with $X_2C{=}CX_2$ **9** (route b) did not result in the desired Sonogashira reaction but in dehydrogenative oxidative coupling of **8b** to form the octatetraynediyl complex **10a**,[18] where the perhaloethene **9** might work as oxidant. The μ-C_8 complex **10a** has already been reported by Lapinte.[4k,l]

(iii) (Hex-3-ene-1,5-diyne-1,6-diyl)diiron Complexes Containing C_6 Spacers and Their Derivatives.[19] The formation of the dinuclear TEE complexes **6** and **7** led us to extend our research targets to the related dinuclear hex-3-ene-1,5-diyne-1,6-diyl system (C_6 bridge) and its longer congener, the octa-3,5-dien-1,7-diyne-1,8-diyl system (C_8 bridge), for which the two synthetic approaches were also feasible (Scheme 4).

(13) Connelly, N.; Gamasa, M. P.; Gimeno, J.; Lapinte, C.; Lastra, E.; Maher, J. P.; Le Narvor, N.; Rieger, A. L.; Rieger, P. H. *J. Chem. Soc., Dalton Trans.* **1993**, 2575.

(14) (a) Rubin, Y.; Knobler, C. B.; Diederich, F. *Angew. Chem., Int. Ed.* **1991**, *30*, 698. (b) Anthony, J.; Boldi, A. M.; Rubin, Y.; Hobi, M.; Gramlich, V.; Knobler, K. B.; Seiler, P.; Diederich, F. *Helv. Chim. Acta* **1995**, *78*, 13. (c) Koentjoro, O. F.; Zuber, P.; Puschmann, H.; Goeta, A. E.; Howard, J. A. K.; Low, P. J. *J. Organomet. Chem.* **2003**, *670*, 178.

(15) Ozawa, T.; Akita, M. *Chem. Lett.* **2004**, 1180.

(16) (a) Sonogashira, K.; Tohda, Y.; Hagihara, N. *Tetrahedron Lett.* **1975**, *50*, 4467. (b) Sonogashira, K. In *Handbook of Organopalladium Chemistry for Organic Synthesis*; Negishi, E., Ed.; Wiley: New York, 2002. (c) Reference 4z. (d) Marsden, J. A.; Haley, M. M. In *Metal-Catalyzed Cross-Coupling Reactions*; de Meijere, A., Diederich, F., Eds.; Wiley-VCH: New York, 2004.

(17) The purple color should arise from a trace amount of the monocationic species $\mathbf{6}^{\bullet+}$ and $\mathbf{7}^{\bullet+}$ presumably resulting from oxidation by adventitious air during the prolonged refluxing.

Scheme 4

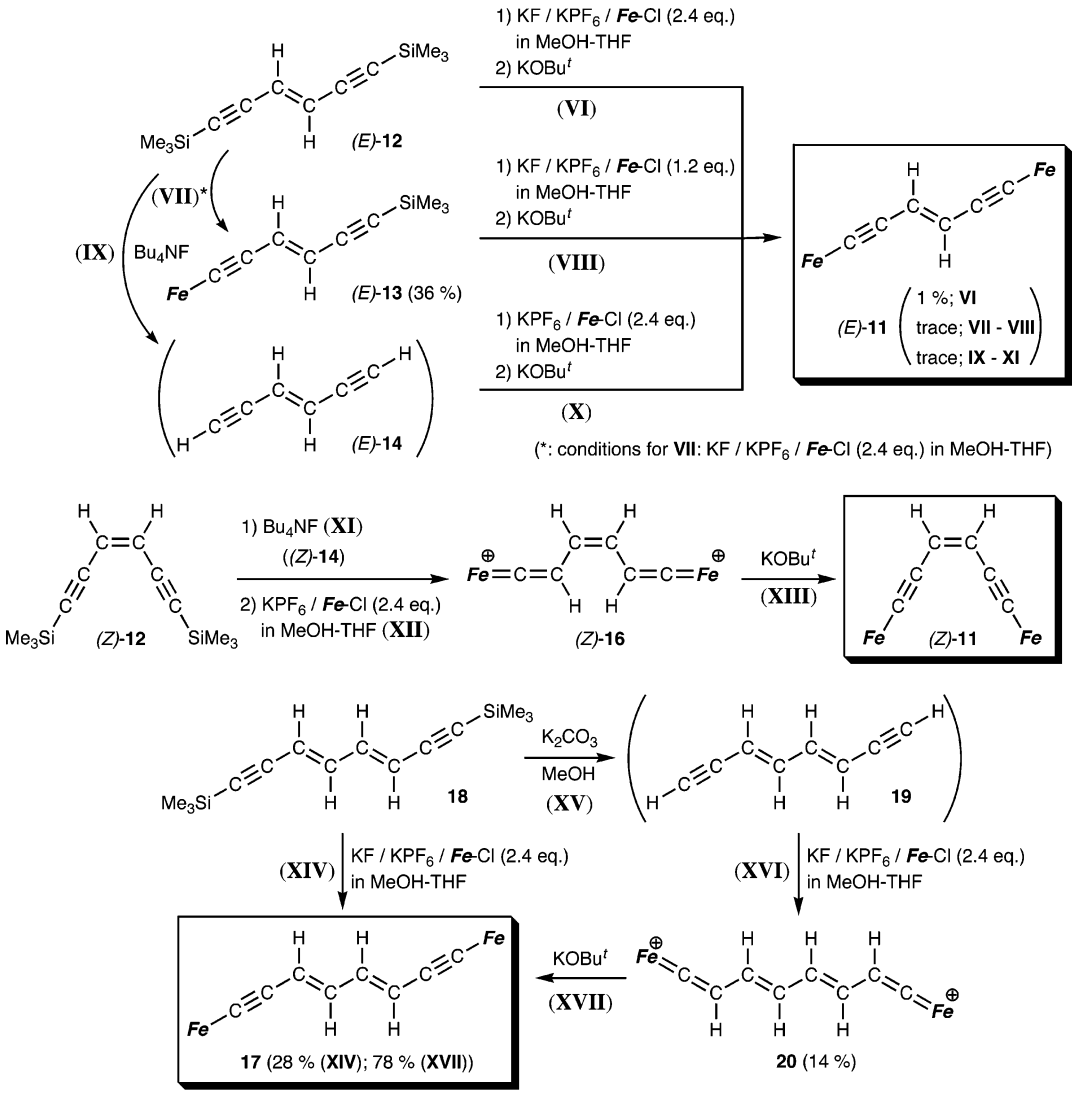

Three routes based on route a were planned for the (*E*)-C_6 complex (*E*)-**11**. The direct (reaction VI) and stepwise Si-substitution of (*E*)-**12** (reactions VII and VIII) gave (*E*)-**11** in very low yields, although the monosubstituted intermediate (*E*)-**13**[18] (reaction VII) was obtained in 36% yield. Then the free 1-alkyne (*E*)-**14** was generated in situ from the corresponding Si precursor (*E*)-**12**[20] according to the procedure reported by Jia (reaction IX)[21f] but subsequent treatment with the Fe reagent (reaction X) gave a mixture containing a trace amount of the desired product (*E*)-**11** along with (*Z*)-***Fe***−C≡C−CH═CHCH═CH_2 (**15**).[18,22]

On the other hand, the desilylation method turned out to be successful for the *Z* isomer ((*Z*)-**11**; reactions XI−XIII) and the extended C_8 complex with the diene part (**17**; reactions XV−XVII), which were derived from the silyl-protected precursors (*Z*)-**12**[20] (via (*Z*)-**16**) and **18**[21d] (via **19**), respectively. The C_8 complex **17** could also be obtained via the direct reaction of **18** with KF−KPF_6 in MeOH−THF (reaction XIV). The vinylidene intermediates (*Z*)-**16** and (*E*,*E*)-**20** could be isolated and characterized by X-ray crystallography as described below. Further extension to the C_{10} system $Me_3Si(C{\equiv}C)_2CH{=}CH(C{\equiv}C)_2SiMe_3$ (**21**) did not afford the desired product, ***Fe***−$(C{\equiv}C)_2CH{=}CH(C{\equiv}C)_2$−***Fe*** (**22**) but a mixture of unidentified

(18) Because the reaction products described in this paper were rather featureless with respect to the spectroscopic data (e.g. one or two unique protons in a molecule of *MW* > 1000, and overlap with the large Ph signals of the dppe ligand), some of the intermediates and products, which could not be characterized spectroscopically, were also subjected to X-ray crystallography when single crystals were available. The crystallographically characterized products are **10a**, (*E*)-**13**, and **15**, and their crystallographic data are shown in the Supporting Information. Selected structural parameters (in Å), Fe═C < cp-Fe═C, < cp-Fe−P1, cp-Fe−P2: 1.751, 120.3, 131.1, 134.0 (**10a**); 1.737, 118.7, 132.7, 131.9; 1.743, 118.6, 130.9, 133.9 ((*E*)-**13** with two independent molecules); 1.748, 120.9, 129.7, 134.2 (**15**).

(19) Recently Ren reported related hex-3-ene-1,5-diyne-1,6-diyl complexes containing a diruthenium fragment as the end caps: Shi, Y.; Yee, G. T.; Wang, G.; Ren, T. *J. Am. Chem. Soc.* **2004**, *126*, 10552.

(20) (a) *E* isomer: Walker, J. A.; Bitler, S. P.; Wudl, F. *J. Org. Chem.* **1984**, *49*, 4733. (b) *Z* isomer: Vollhardt, K. P. C.; Winn, L. S. *Tetrahedron Lett.* **1985**, *26*, 709. For the deslilylated compound **14**, see: (c) Figeys, H. P.; Gelbke, M. *Tetrahedron Lett.* **1970**, 5139.

(21) (a) Etzenhouser, B. A.; Cavanaugh, M. D.; Spurgeon, H. N.; Sponsler, M. B. *J. Am. Chem. Soc.* **1994**, *116*, 2221. (b) Etzenhouser, B. A.; Chen, Q.; Sponsler, M. B. *Organometallics* **1994**, *13*, 4176. (c) Sponsler, M. B. *Organometallics* **1995**, *14*, 1920. (d) Chung, M.-C.; Gi, X.; Etzenhouser, B. A.; Spuches, A. M.; Rye, P. T.; Seetharaman, S. K.; Rose, D. J.; Zubieta, J.; Sponsler, M. B. *Organometallics* **2003**, *22*, 3485. (e) Liu, S. H.; Chen, Y.; Wan, K. L.; Wen, T. B.; Zhou, Z.; Lo, M. F.; Williams, I. D.; Jia, G. *Organometallics* **2002**, *21*, 4984. (f) Liu, S. H.; Xia, H.; Wen, T. B.; Zhou, Z.; Jia, G. *Organometallics* **2003**, *22*, 737. (g) Liu, S. H.; Hu, Q.; Xue, P.; Wen, T. B.; Williams, I. D.; Jia, G. *Organometallics* **2005**, *24*, 769 and references therein. (h) Klein, A.; Lavastre, O.; Fiedler, J. *Organometallics* **2006**, *25*, 635.

Scheme 5

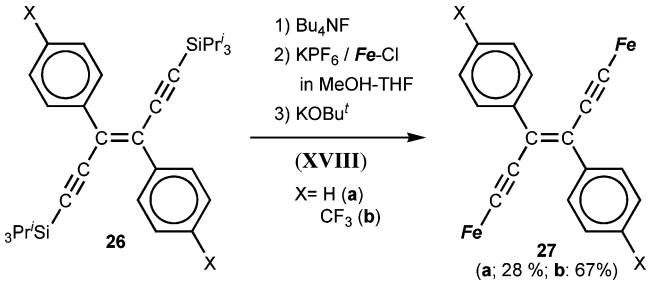

products. In these cases as well, Sonogashira coupling was unsuccessful.[23]

(iv) Diaryl-Substituted C_6 Complexes 27. To study the substituent effect of the olefinic part, the diaryl-substituted C_6 complexes **27** were prepared via route a (Scheme 5): i.e., metalation of the free diyne compounds (generated in situ from the $SiPr^i_3$ precursor **26**) with the iron reagent followed by deprotonation with $KOBu^t$ (**XVIII**). The reaction was dependent on the substituent (X): i.e., the reaction of the substrate **26** with an electron-withdrawing substituent (**26b**) proceeded smoothly compared to that of **26a** (X = H). Attempted reactions of the *p*-Me and *p*-OMe derivatives were sluggish and afforded inseparable mixtures of products.

Comments on the Synthesis of 2D Polyiron Complexes. 2D polyiron complexes are not always easily accessible, as described above, owing to (1) the bulky ***Fe*** group hindering multiple metalation and (2) the limited synthetic access.

The first problem may be overcome by using a spacer even longer than the C≡C−C≡C bridge, and in fact, we recently succeeded in preparation of a tetrairon complex with ethynylated phenylene linkers, (***Fe***−C≡C-*p*-C_6H_4)$_2$C═C(*p*-C_6H_4C≡C−***Fe***)$_2$.[24] However, the use of such a long linker causes another problem; the communication becomes worse as the metal centers are separated.

As for the second, synthetic problem, the vinylidene method (route a) is effective for introduction of a C≡C−R group (e.g. **I** and **III**) but cannot be always extended to the introduction of a C≡C−C≡C−R group (e.g., reactions of **4** and **21**; see above). Although the reason is not clear, the failure could be ascribed to the stability of the intermediate. In the case of the C≡C−R system, the vinylidene intermediate ([***Fe***═C═C(H)R]$^+$) is the only possible intermediate, whereas, in the case of the C≡C−C≡C−R system, another intermediate such as [***Fe***═C═C═C═C(H)R]$^+$ may be formed in addition to the desired [***Fe***═C═C(H)-C≡C−R]$^+$ species, perhaps leading to decomposition if it is unstable.[25]

Spectroscopic and Crystallographic Characterization of the Obtained Iron Complexes. (i) Diiron Complexes. The obtained diiron complexes **6**, **7**, (*E*)- and (*Z*)-**11**, and **17** were characterized by spectroscopic and/or crystallographic methods. Their spectroscopic data are summarized in Table 1. Symmetrical, disubstituted olefin structures are evident from the NMR data: i.e., (1) single sets of NMR resonances for the Cp* (^{1}H) and dppe ligands (^{31}P) and the substituents on the olefinic moiety (^{1}H) and (2) the intensities of ^{1}H NMR signals for the Cp* ligand and the substituents. The presence of a C≡C group is evident from the IR absorptions around 2000 cm^{-1}. The configuration of the olefinic part was confirmed by X-ray crystallography.

Table 1. Selected Spectroscopic Data for Diiron Complexes

complex	^{1}H NMR (δ_H/ppm)[a] C_5Me_5	^{1}H NMR (δ_H/ppm)[a] ═CH/others[c]	^{31}P NMR (δ_P/ppm)[a]	IR[b] ($\nu_{C\equiv C}$/cm^{-1})
6	1.60	0.22 ($SiMe_3$)	94.5	2128, 2021
7	1.58	2.73 (≡CH)	93.8	2095, 2044, 2023[d]
(*E*)-**11**	1.50	5.77	93.6	2036, 2011
(*Z*)-**11**	1.23	5.45	93.5	2024
(*Z*)-**16**[e]	1.48	4.72 (m), 4.06 (dd, 7.2, 1.6)	85.1	
(*E*,*E*)-**17**	1.52	6.03 (d, 13.4), 6.50 (dd, 13.4, 2.1)	93.2	2018
20[e]	1.49	4.94 (m), 5.12 (m), 5.24 (dd, 13.7, 2.5)	88.5	
27a	1.35		93.3	2016
27b	1.26		93.3	2023

[a] ^{1}H (at 200 MHz) and ^{31}P NMR (at 83 MHz) were recorded in C_6D_6 unless stated. [b] Recorded as KBr pellets. [c] Coupling patterns and coupling constants (in Hz) are shown in parentheses. [d] $\nu_{\equiv C-H}$: 3318 cm^{-1}. [e] NMR in CD_3CN.

Molecular structures of the diiron complexes **6**, **7**, and **17** were determined by X-ray crystallography, and their ORTEP views and selected structural parameters are shown in Figure 1 and Table 2, respectively. The three-legged piano-stool configuration of the iron centers is evident from the bond angles defined by the ligands and cp (the centroid of the Cp* ligand), and no significant difference is observed for the series of the complexes listed in Table 2.

For the TEE complexes **6** and **7**, disorder is noted for the central olefinic parts, which sit on centrosymmetric sites, and this type of disorder is frequently observed for TEE derivatives, including **4**, as previously reported by us.[15] While the disorder hampers a detailed discussion on the bridging organic moiety, (1) clear bond alternation is evident, (2) the *E* configuration has been confirmed, and (3) structures of the core parts of **6** and **7** are essentially the same. Structural parameters for the acetylide parts are comparable to those of related mononuclear complexes, including **10a**, (*E*)-**13**, and (*Z*)-**15**.[18] From the overviews it is apparent that the bulky ***Fe*** groups hinder introduction of the third and fourth ***Fe*** groups.

E−*Z* isomerization was noted for the diene part in **17**. When a C_6D_6 solution of **17** left at room temperature was monitored by ^{1}H NMR (Cp* region; Figure 2), the single Cp* resonance for the *E*,*E* isomer was partially converted to a pair of two singlets assignable to the *E*,*Z* isomer and then to the single resonance for the *Z*,*Z* isomer, and an equilibrium with a composition of 60 (*E*,*E*):22 (*E*,*Z*):18 (*Z*,*Z*) was finally attained. The isomers can also be characterized by the ^{1}H NMR data for the olefinic parts and the ^{31}P NMR data (*E*,*E* isomer, δ_H 6.03, 6.53 (2H (doublet) × 2), δ_P 93.19; *E*,*Z* isomer, δ_H 6.77 (1H, m), 5.77 (1H, m) (the other signals were not located), δ_P 93.63, 93.35; *Z*,*Z* isomer, δ_H 6.20, 5.61 (2H (doublet) × 2), δ_P 93.24) (Figure 2c). The *E*,*E* configuration of the major isomer was also verified on the basis of the large CH═CH coupling constants for a simulated spectrum (CH_A═CH_B-CH_C═CH_D: $^3J_{AB}$ = $^3J_{CD}$ = 14.35 Hz, $^4J_{AC}$ = $^4J_{BD}$ = −0.69 Hz, $^5J_{AD}$ = 0.71 Hz, $^3J_{BC}$ = 11.50 Hz; $^5J_{P-H(A,D)}$ = 1.80 Hz, $^6J_{P-H(B,C)}$ = 0.90 Hz). The stereoisomerism was also noted by an X-ray crystallographic analysis (Figure 1c). Initial refinement based on the single component (*E*,*E* isomer) resulted in large B_{eq} values for the central olefinic carbon atoms, but the refinement was

(22) The formation mechanism of **15** is unknown.

(23) A 2:1 reaction between ***Fe***−C≡C−H (**8a**) and the 1,2-dihaloethene (X)HC═CH(X) (**23**) resulted in a complicated mixture of products. On the other hand, a 1:1 reaction gave the monosubstituted product ***Fe***−C≡C−CH═CHX (**24**: X = (*E*)-Cl (**24a**; 37%); X = (*E*)- and (*Z*)-Br (**24b**; 22%)), but the repeated alkynylation of **24** did not result in the substitution but in a mixture of unidentified products (X = Cl) or dehydrogenative oxidative coupling of **8a** giving the μ-C_4 complex **10b**[4b,c] (X = Br), where the halide **24b** worked as oxidant to be converted to the reduced product ***Fe***−C≡C−CH═CH_2 (**25**).

(24) Tanaka, Y.; Ozawa, T.; Inagaki, A.; Akita, M., submitted.

(25) Bruce, M. I. *Chem. Rev.* **1998**, *98*, 2797; **1991**, *91*, 197.

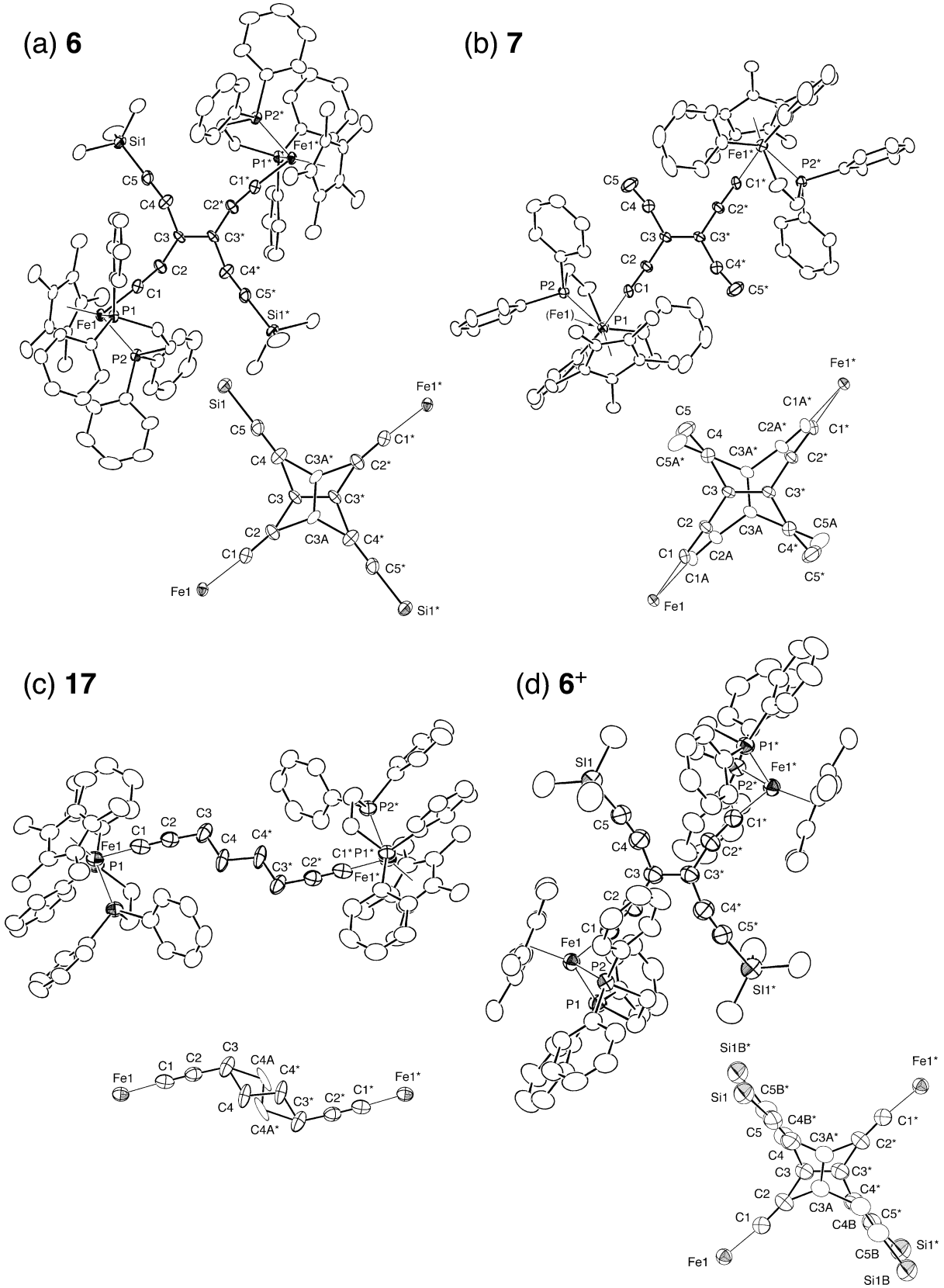

Figure 1. ORTEP views of the diiron acetylide complexes (a) **6**, (b) **7**, (c) **17**, and (d) the cation of $\mathbf{6}^{+}PF_6^{-}$ drawn with thermal ellipsoids at the 30% probability level. The disordered core parts are also shown.

successfully achieved by taking into account the *E,E* and *Z,Z* isomers with a composition of 66:34. It is surprising that linkers with different configurations span the two metal centers separated at the same distance, suggesting flexibility of the olefinic linker. *E*−*Z* isomerization is a problem, which can be associated with olefinic linkers, and the present result provides an example for this problem. This problem could be avoided by using cyclic dienes with a fixed *s-cis-E,E* configuration such as a thiophene linker.[4s] No evidence for stereoisomerism was observed for the mono-olefinic complexes **6**, **7**, and **11**; the *E*

Table 2. Selected Structural Parameters for Diiron Complexes[a]

	6	**7**	**6**$^+PF_6^-$	**17**	**16**	**20**
Fe···Fe	9.923(1)	9.8944(5)	9.848(4)	11.778(2)	9.214(1)	11.6260(5)
Fe1−P1	2.159(1)	2.1751(5)	2.202(1)	2.187(2)	2.219(1)	2.238(2)
Fe1−P2	2.166(2)	2.1711(7)	2.204(1)	2.186(2)	2.235(1)	2.207(2)
Fe−C(Cp*)	2.098(4)−2.130(5)	2.096(2)−2.134(2)	2.117(4)−2.153(4)	2.096(6)−2.137(6)	2.132(4)−2.175(4)	2.113(6)−2.176(6)
Fe−cp[b]	1.741	1.741	1.756	1.740	1.780	1.776
Fe1−C1	1.878(5)	1.858(9)	1.841(4)	1.896(7)	1.740(4)	1.723(6)
C1−C2	1.212(6)	1.249(9)	1.231(6)	1.227(9)	1.329(5)	1.321(8)
C2−C3	1.443(7)	1.427(4)	1.423(8)	1.43(1)	1.412(9)	1.428(9)
C3−C3A*	1.35(2)	1.370(5)	1.34(1)		1.36(1)	
C3−C4	1.479(9)	1.440(4)	1.47(2)	1.41(1)		1.348(8)
C4−C5	1.217(8)	1.164(9)	1.19(2)			
others	1.827(6) (C5−Si1)		1.84(2) (C5−Si1)	1.51(3) (C4−C4*)		1.41(1) (C4−C4*)
cp−Fe1−C1[b]	119.6	121.2	119.9	120.7	120.6	119.9
cp−Fe1−P1[b]	134.7	131.4	130.9	130.0	130.4	130.3
cp−Fe1−P2[b]	131.2	134.1	131.7	134.7	129.6	134.7
C1−Fe1−P1	83.9(1)	84.1(3)	90.5(1)	85.2(2)	89.7(1)	92.0(2)
C1−Fe1−P2	86.3(2)	82.0(2)	83.2(1)	84.1(2)	87.5(1)	86.3(2)
P1−Fe1−P2	84.50(5)	86.14(2)	85.82(5)	85.63(6)	85.96(4)	85.48(6)
Fe1−C1−C2	176.4(5)	174.2(7)	172.6(4)	177.8(6)	174.4(3)	171.4(5)
C1−C2−C3	163.0(7)	176.6(5)	167.1(5)	175.9(5)	125.0(5)	124.2(5)
C2−C3−C3A*	120.3(8)	122.9(4)	122.5(8)		126.2(7)	
C3*−C3−C4	113.3(7)	119.3(3)	111(1)			
C2−C3−C4	126.3(7)	117.8(3)	123.5(8)	108.6(8)		125.3(5)
C3−C4−C5	164.0(6)	167.7(3)	166(2)			
others	176.2(6) (C4−C5−Si1)		170(1) (C4−C5−Si1)	116(1) (C3−C4−C4*)		124.9(6) (C3−C4−C4*)
θ/θ'[c]	1 (0)/0(1)[d]	1.5(6)/1(2)[e]	19(1)/12(1)[f]			

[a] Interatomic distances in Å and bond angles in deg. [b] Centroid of the Cp* ring. [c] Dihedral angles of the olefinic part. [d] C2−C3−C3*−C4*/C2−C3A−C3A*−C4. [e] C2−C3−C3*−C4*/C2A−C3A−C3A*−C4. [f] C2−C3−C3*−C4B.

Scheme 6

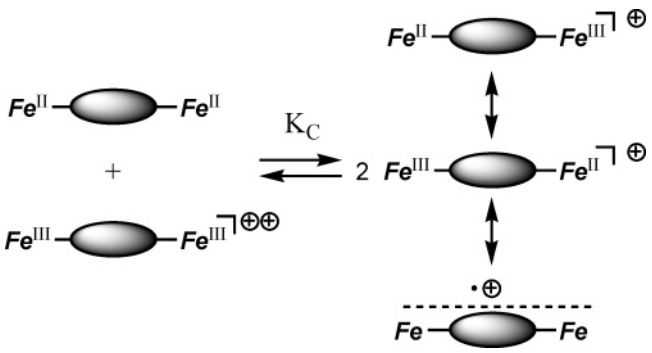

and *Z* isomers of **11** are distinguishable by their spectroscopic features (Table 1) and show discernible electrochemical features (see below).

(ii) Vinylidene Intermediates. The isolated vinylidene intermediates showed the characteristic highly deshielded C_α signals (^{13}C NMR) coupled with the two P nuclei (triplet; δ_C 368.2 ((*Z*)-**16**) and 367.2 ((*E*,*E*)-**20**))[4c,25] and were also characterized by X-ray crystallography (Figure 3 and Table 2). The structure of the vinylidene linkage (Fe═C═C) is evident from the bond alternation pattern, which is different from those observed for the Fe−C≡C moieties in the acetylide complexes described above. The three-legged piano-stool structure of the ***Fe*** parts is similar to that of the acetylide complexes, whereas the slightly elongated Fe−ligand (P and cp) distances can be ascribed to decreased back-donation to the ligand caused by the π-acidic vinylidene ligand as well as the formal positive charge on the metal center. The *Z* configuration of the diene moiety in (*Z*)-**16** reveals that reactions XI−XIII proceed with retention of the configuration, while the molecule is disordered with respect to the crystallographic centrosymmetric inversion center, as shown in Figure 3a. (*E*)-**16** could be also isolated from reaction VI (without addition of KOBu^t) and characterized by its NMR data.[26]

Performance as Molecular Wires. The performance of the obtained diiron complexes as molecular wires was evaluated on the basis of their electrochemical properties and near-IR observation of their monocationic radical species resulting from one-electron oxidation.

(i) Cyclic Voltammetry of Diiron Complexes. The extent of delocalization over a π-conjugated system can be conveniently evaluated on the basis of the comproportionation constant (K_C), the equilibrium constant between a mixed-valence state and two different non-mixed-valence states (Scheme 6).[27] In the system with a large K_C value, delocalization of the unpaired electron of the 1e-oxidized species over the π-conjugated system leads to a stable mixed-valence state. The K_C value can be determined according to the equation $K_C = \exp[(\Delta E)F/RT]$, where ΔE stands for the separation of the first and second oxidation processes ($\Delta E = |E_{1/2}^1 - E_{1/2}^2|$ (in V)). Electrochemical data for **6**, **7**, (*E*)- and (*Z*)-**16**, (*E*,*E*)-**17**, and **27a**,**b** are summarized in Table 3, and cyclic voltammograms for selected iron complexes are shown in Figure 4. The voltammograms contain two reversible redox waves, as judged by (1) i_c/i_a values close to unity and (2) $E_a - E_c$ separations close to the ideal value (57 mV at 298 K), and large K_C values on the order of 10^8−10^9 (Table 3) calculated from the separations as large as 556 mV reveal that the diiron complexes are efficient molecular wires belonging to class III according to the Robin and Day classification.[28]

(ii) Preparation of Mono- and Dicationic Diiron Complexes. The two well-separated reversible redox processes of the diiron complexes **6**, **7**, (*E*)- and (*Z*)-**11**, **17**, and **27a**,**b**

(26) δ_H (CD_3CN): 7.7−7.1 (m, Ph), 4.52, 4.02 (2H × 2, m, ═CH), 2.8, 2.4 (2H × 2, m, PCH_2), 1.24 (30H, s, Cp*). δ_P (CD_3CN): 89.2.

(27) For detailed discussions, see, for example, refs 4a,c, 6a, and 21a,b.

(28) A significant solvent effect was noted. Geiger et al. recently pointed out the critical dependence of K_C on the solvent and electrolyte: Barriére, F.; Geiger, W. E. *J. Am. Chem. Soc.* **2006**, *128*, 3980 and references therein.

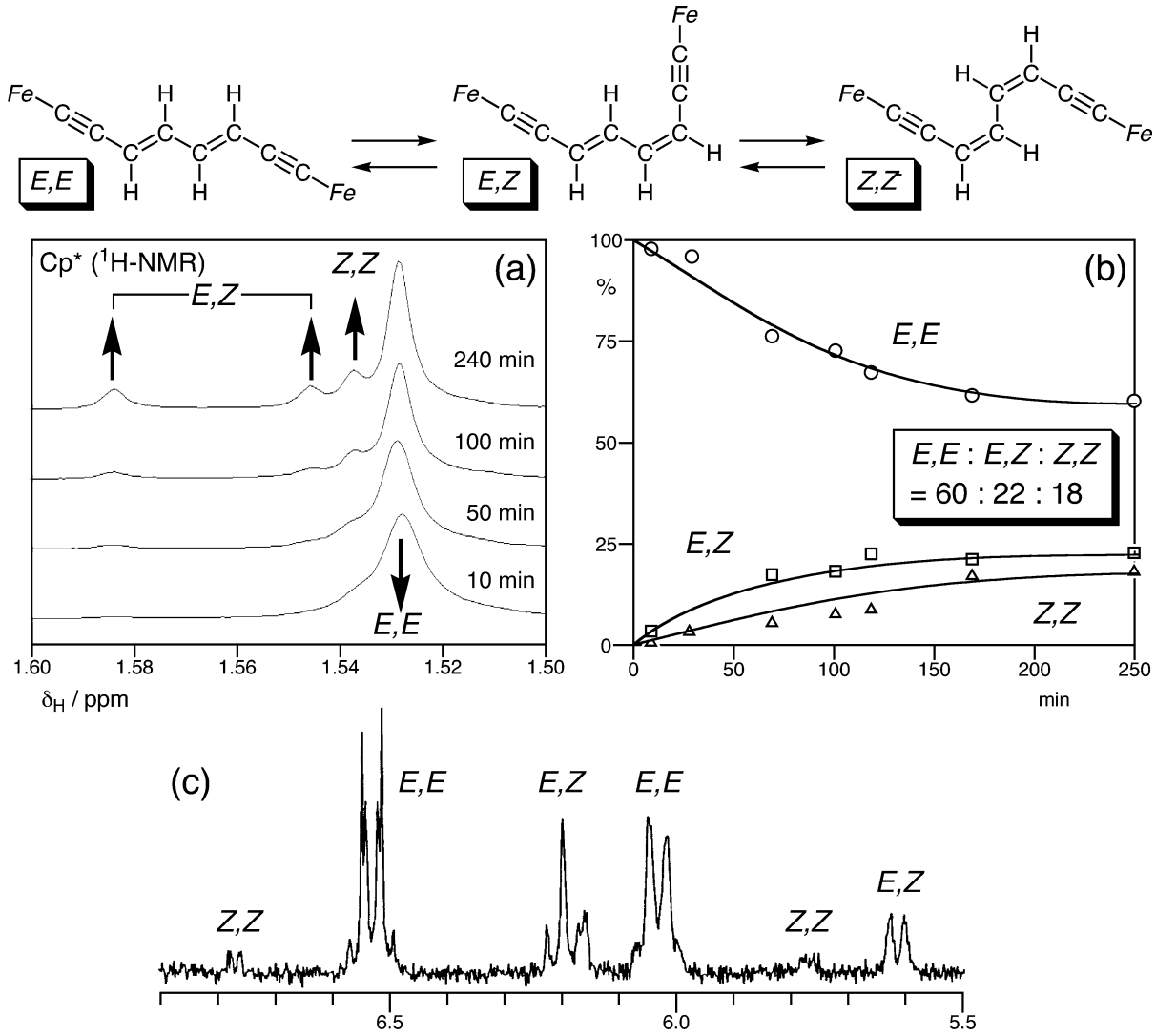

Figure 2. ^{1}H NMR monitoring of the isomerization of (*E*,*E*)-**17** (observed in C_6D_6): (a) changes in the Cp* region; (b) plots of the isomer ratio as a function of time; (c) olefinic region of an equilibrated isomeric mixture.

Scheme 7

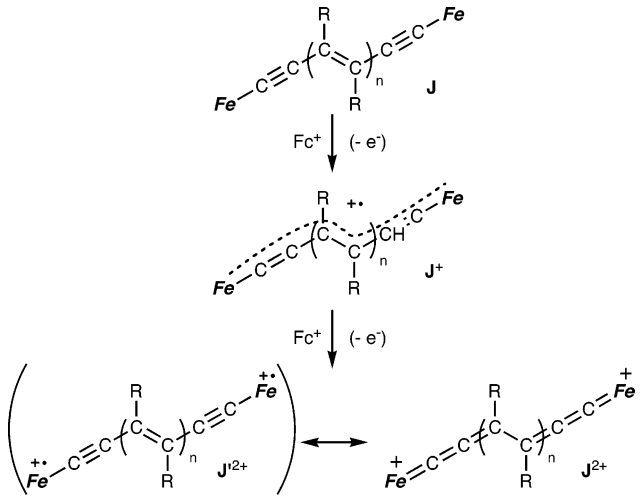

suggested that the monooxidized species might be stable enough to be isolated and characterized. In addition, an intervalence charge-transfer band for the isolated monocationic radical species provides another measure for the performance as molecular wires. Treatment of the diiron complexes **J** with 0.9 or 1.9 equiv of $FcPF_6$ (Fc = $FeCp_2$) in THF gave stable mono- ($\mathbf{J}^+PF_6^-$) and dicationic complexes ($\mathbf{J}^{2+}(PF_6^-)_2$), respectively (Scheme 7). The oxidized species traced the same cyclic voltammogram as the corresponding neutral counterparts. IR and UV−vis−near-IR spectra for the representative examples are compared in Figure 4 together with the CV traces.

The monocationic, odd-electron species ($\mathbf{J}^+$) are paramagnetic, and their intense $\nu_{C\equiv C}$ vibrations (Figure 4 and Table 3) appearing in the energy region lower than those of the neutral counterparts reveal that delocalization of the unpaired electron over the metal−carbon linkages ($\mathbf{J}^+$ in Scheme 7) causes a decrease in the bond order of the C≡C parts.

The monooxidized species of **6** ($\mathbf{6}^+PF_6^-$) could also be characterized by X-ray crystallography (Figure 1d). Although the two independent disorder problems associated with the central olefinic moiety and the $Me_3SiC\equiv C$ part hampered detailed discussion of the structure, the molecular structure could be verified. The geometrical parameters of $\mathbf{6}^+$ are roughly comparable to those of the neutral counterpart **6** as compared in Table 3, but the bond alternation in $\mathbf{6}^+$ becomes less apparent compared to that in **6**, in accord with the delocalized resonance structures $\mathbf{J}^+$ shown in Scheme 7. In particular, shortening of the Fe−C distance (1.841(4) Å; cf. **6**, 1.878(5) Å) clearly indicates its multiple-bond character. In addition, a decrease of the bond order of the central C═C moiety causes a significant

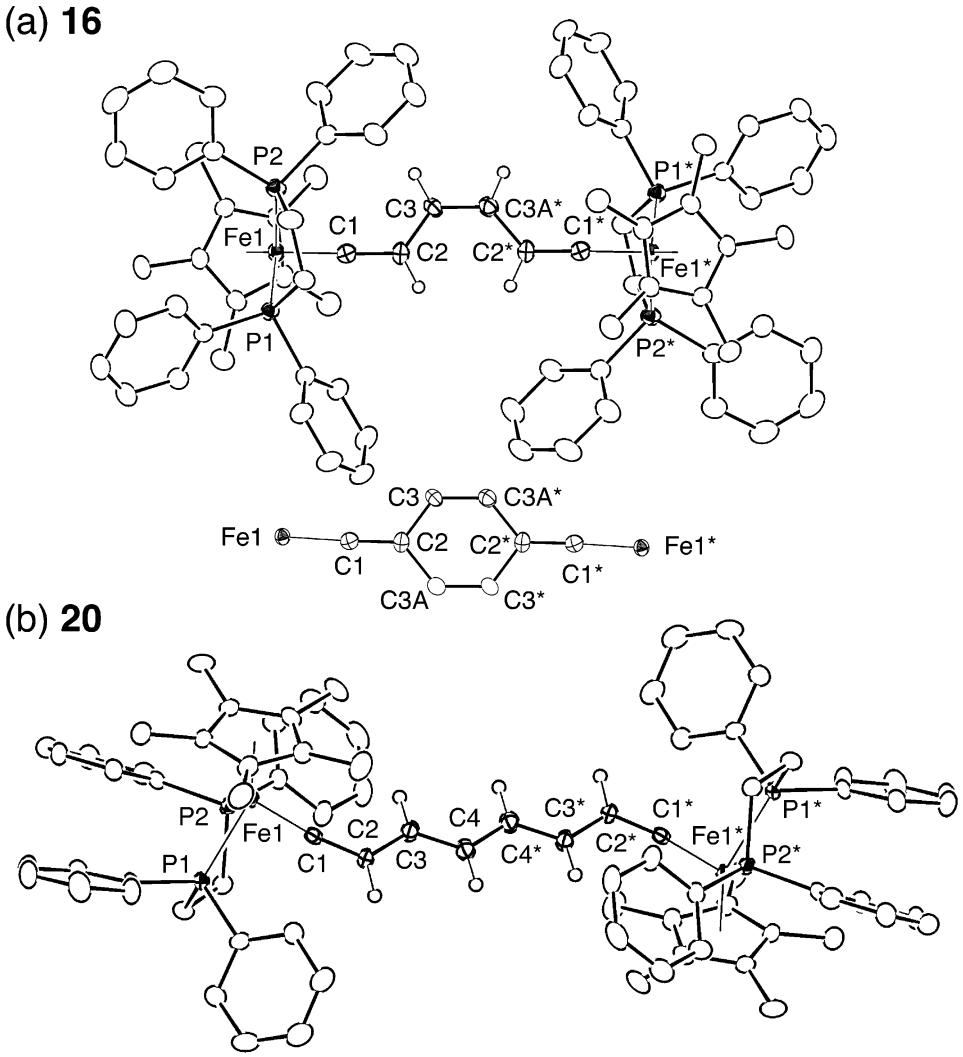

Figure 3. ORTEP views of the cations of the cationic diiron vinylidene complexes (a) (*Z*)-**16** and (b) **20** drawn with thermal ellipsoids at the 30% probability level. The disordered core part of (*Z*)-**16** is also shown.

Table 3. Electrochemical, Near-IR, and IR Data for the Monocationic Diiron Complexes *Fe*−C≡CC(R)═C(R)C≡C−*Fe*[a]

	electrochemical data[b]					IVCT band (near-IR) for monocation[d]				
complex (R)	$E_{1/2}$/mV	$\|E_a - E_c\|$/mV	i_c/i_a	ΔE/mV	K_C[c]	ν_{max}/cm^{-1} (ϵ/M^{-1} cm^{-1})	$\nu_{1/2}$/cm^{-1} (r/Å)[f]	$\nu_{1/2}^{calcd}$/cm^{-1} [e]	V_{ab}^{II},[g] V_{ab}^{III} [h]/eV	$\nu_{C\equiv C}$/cm^{-1} [i]
6[e] (C≡C−SiMe$_3$)	−930	49	1.0	522	6.8×10^8	5910 (1.32×10^4)	2249 (9.85)	3695	0.11, 0.36	2128, 1968, 1884
	−408	61	1.1							
7[e] (C≡CH)	−907	57	1.0	499	2.7×10^8	5695 (2.27×10^3)	2675 (9.85)	3627	0.048, 0.35	1954, 1890
	−408	64	1.0							
(*E*)-**11** (H)	−1021	54	0.9	492	2.1×10^8					
	−529	62	1.0							
(*Z*)-**11** (H)	−989	54	0.9	477	1.2×10^8	6305 (1.60×10^4)	2488 (9.85)	3961	0.13, 0.39	1995, 1893
	−513	63	1.2							
(*E*,*E*)-**17**[j]	−871	49	0.9	276	4.7×10^4	5181 (5.65×10^3)	2664 (11.78)	3459	0.060, 0.32	1970, 1904
	−595	57	1.0							
27a (C$_6$H$_5$)	−1092	84	1.0	536	1.4×10^9	6427 (2.2×10^4)	1905 (9.85)	3853	0.13, 0.40	1980, 1892
	−557	75	0.9							
27b (*p*-CF$_3$C$_6$H$_4$)	−972	62	1.0	556	3.0×10^9	6266 (1.9×10^4)	1769 (9.84)	3805	0.12, 0.39	1980, 1893
	−417	57	0.9							

[a] ***Fe*** = FeCp*(dppe). [b] Conditions: [complex] = ~2×10^{-3} M, [Bu$_4$NPF$_6$] = 0.1 M, in CH$_2$Cl$_2$, at 278 K, scan rate 100 mV/s. [c] $K_C = \exp[38.97(\Delta E)]$ (at 298 K). [d] Observed in CH$_3$CN. [e] $\nu_{1/2}^{calcd} = (2310\nu_{max})^{1/2}$. [f] r for the C$_6$ complexes is taken from the Fe···Fe separation of the cation **6**$^+$, and that for the C$_8$ complex is taken from the neutral (*E*,*E*)-**17**. [g] V_{ab}^{II} (estimated as a class II compound) = $(2.55 \times 10^{-6})(\nu_{max}\epsilon_{1/2})^{1/2}r^{-1}$ (eV). [h] V_{ab}^{III} (estimated as a class III compound) = $(1/2)\nu_{max}$ (cm^{-1}) = $(6.20 \times 10^{-5})\nu_{max}$ (eV). [i] For monocations; observed as KBr pellets. [j] ***Fe***−C≡CCH═CHCH═CHC≡C−***Fe***.

distortion of the olefinic part from a planar structure, as can be seen from the dihedral angles θ and θ' (>10°; cf. θ/θ' for **6** and **7**, ~0). The Fe−ligand (dppe and cp) distances in the monocationic species **6**$^+$ are between those of the neutral species **6** and the dicationic vinylidene species **16** and **20**, supporting the discussion on the elongation based on the decreased back-donation in cationic species (see above).

The dicationic species (**J**$^{2+}$) are diamagnetic, as indicated by their NMR signals appearing in the normal diamagnetic region,[29] indicating that the two unpaired electrons (**J′**$^{2+}$) couple with each other to lead to the cumulenic structure (**J**$^{2+}$) as the dominant resonance contributor. The cumulenic structure is

(29) Complexes **6** and **7** showed slightly broad NMR spectra, but the signals appeared in the normal range.

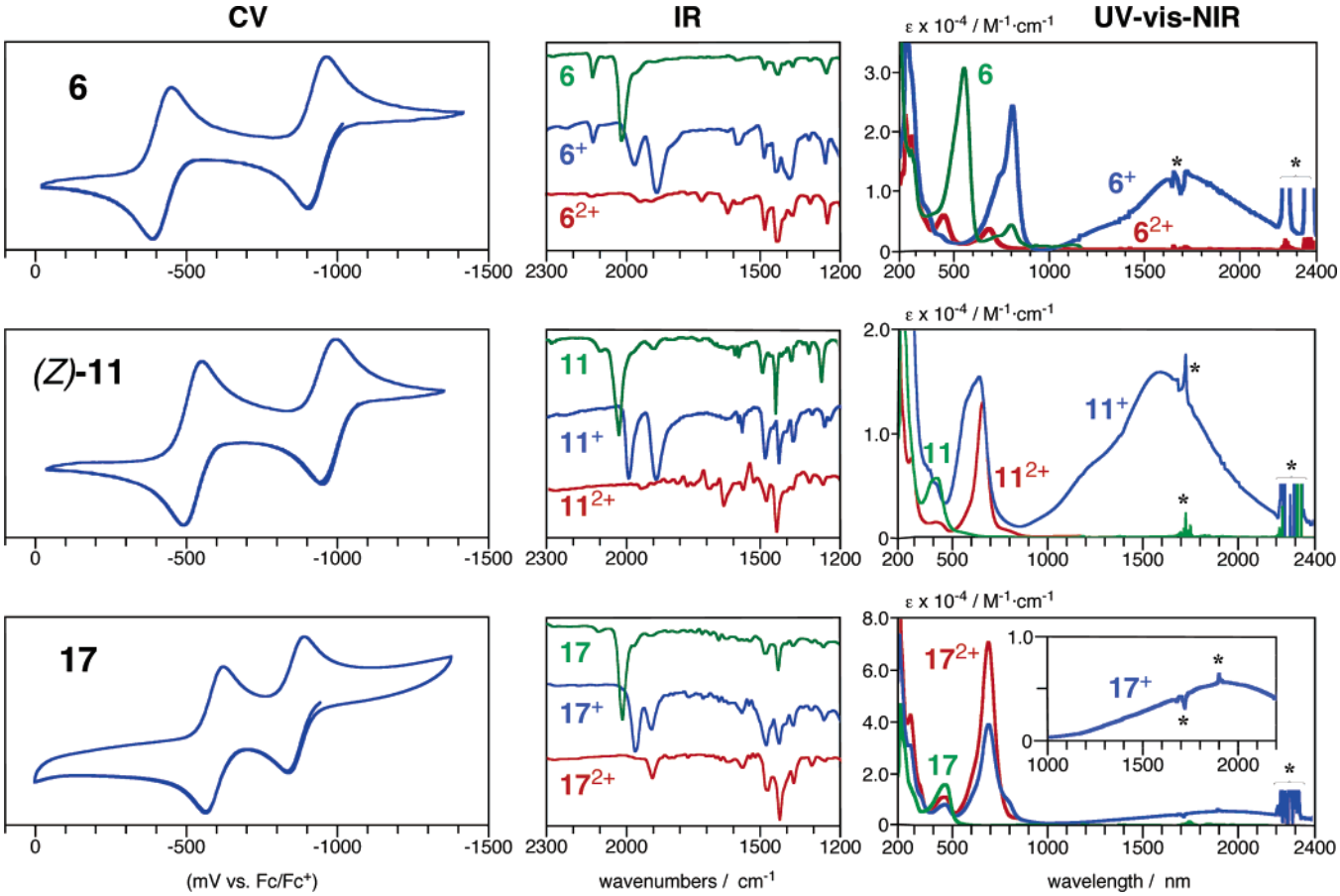

Figure 4. Cyclic voltammograms, IR spectra, and UV−vis−near-IR spectra of selected diiron complexes. (the asterisks denote solvent noises).

supported by the disappearance of the $\nu_{C\equiv C}$ vibrations (Figure 4) as well as the highly deshielded ^{13}C NMR signals (e.g. δ_C 286.4 ((*Z*)-**11**$^{2+}$), 274.0 (**17**$^{2+}$)) characteristic of the α-carbon atom of cumulenylidene metal complexes.[6a,25]

(iii) Near-IR Spectra of One-Electron-Oxidized Species.[27] The stability of the mixed-valence monocation obtained by one-electron oxidation of the neutral compound can be estimated on the basis of the K_C value obtained by electrochemical analysis (see above). Furthermore, in case the monocation is stable enough to be isolated, it can be subjected to near-IR measurement. A mixed-valence monocation shows a broad intense intervalence charge transfer (IVCT) band in the near-IR region, which is assigned as the $\pi-\pi$ transition peculiar to such a highly delocalized system. The effective electronic coupling parameter V_{ab} is another measure for the stability of the delocalized system and can be obtained on the basis of the spectroscopic parameters of the absorption. The V_{ab} value for class II Robin-Day compounds can be calculated according to the Hush formula: $V_{ab} = (2.55 \times 10^{-6})(\nu_{max}\epsilon\nu_{1/2})^{1/2}r^{-1}$ (in eV), where ν_{max}, ϵ, $\nu_{1/2}$, and r denote the absorption maximum, absorption coefficient, half-height width, and distance between the two redox active centers, respectively. On the other hand, for class III Robin-Day compounds, for which the half-height width ($\nu_{1/2}$) is narrower than the critical value $(2310\nu_{max})^{1/2}$ (in cm^{-1}), the electronic coupling can be evaluated using the equation $V_{ab} = (1/2)\nu_{max}$ (in cm^{-1}) $= 6.20 \times 10^{-5}\ \nu_{max}$ (in eV). Although no theoretical relationship between the K_C and V_{ab} values is established, an efficient molecular wire shows larger K_C and V_{ab} values.

Near-IR data for the isolated monocations are summarized in Table 3. The monocationic species show broad intense IVCT bands in the near-IR region (∼1500 nm; Figure 4), in contrast to the neutral and dicationic species, which are silent in that region. For comparison, two values (V_{ab}^{II} (calculated as assumed to be class II) and V_{ab}^{III} (calculated as assumed to be class III)) are given in Table 3. The metal−metal separation (r) for the C_6 complexes is taken from that of **6**$^+$PF$_6^-$, and that for the C_8 complex **17**$^+$ is taken from the neutral counterpart **17**. In all cases, (i) the $\nu_{1/2}$ values are smaller than the critical values and (ii) the large V_{ab} values support the notion that the complexes are efficient molecular wires belonging to class III, in accord with the electrochemical evaluation discussed above.[30]

(iv) Evaluation of the Performance of the Diiron Complexes as Molecular Wires. The K_C and V_{ab} values for the obtained complexes are compared with those of the related complexes reported previously by Lapinte and Sponsler (Table 4). As for the complexes obtained by the present study, the trend observed for the K_C values are essentially the same as those observed for the V_{ab}^{II} and V_{ab}^{III} values. The following discussion, therefore, is based on the K_C values for the sake of simplicity.

The K_C values for the C_6 complexes **6**, **7**, **11**, and **27** are in the range of $(0.12-3.0) \times 10^9$, close to the region for class III Robin−Day compounds, while the K_C value for the C_8 complex **17** diminishes by the order of 10^{-5}. The dependence of K_C on r was already pointed out by Gladysz[6c] and Lapinte (e.g. see **30**−**32** in Table 4);[4] the K_C value diminishes exponentially as a function of the distance between the two metal centers: i.e., the number of the carbon atoms spanning the two redox-active metal centers.

(30) The ν_{max} values were not dependent on the solvent polarity (e.g. (*Z*)-**11**: ν_{max}= 6250 cm^{-1} (in CH_2Cl_2), 6305 cm^{-1} (MeCN)), supporting the classification as class III.[27]

Table 4. Comparison of the K_C and V_{ab} Values for Diiron Complexes

X in ***Fe***−C≡CXC≡C−***Fe***[a]		n[b]	K_C[c]	V_{ab}^{II}/eV[d]	V_{ab}^{III}/eV[e]	ref
$(Me_3SiC{\equiv}C)C{=}C(C{\equiv}CSiMe_3)$	**6**	6	6.8×10^8	0.11	0.36	*f*
$(HC{\equiv}C)C{=}C(C{\equiv}CH)$	**7**	6	2.7×10^8	0.048	0.35	*f*
HC=CH	(*E*)-**11**	6	2.1×10^8			*f*
HC=CH	(*Z*)-**11**	6	1.2×10^8	0.13	0.39	*f*
(Ph)C=C(Ph)	**27a**	6	1.4×10^9	0.13	0.40	*f*
$(p\text{-}CF_3C_6H_4)C{=}C(p\text{-}C_6H_4CF_3)$	**27b**	6	3.0×10^9	0.12	0.39	*f*
HC=CHHC=CH	(*E*,*E*)-**17**	8	4.7×10^4	0.060	0.32	*f*
Y in ***Fe***−Y−***Fe***[a]		n[b]	K_C[c]	V_{ab}^{II}/eV[d]	V_{ab}^{III}/eV[e]	ref
CH=CHCH=CH	**28**	4	1.5×10^{10}	0.24	0.49	21a
C(OMe)=CH−CH=C(OMe)	**29**	4	2.2×10^7	0.11	0.54	4a,w
C≡CC≡C	**30**	4	1.6×10^{12}	0.19	0.47	4b,c
C≡CC≡CC≡C	**31**	6	1.0×10^9			4a
C≡CC≡CC≡CC≡C	**32**	8	2.0×10^7	0.32	0.12	4k,l
$C{\equiv}CC_4H_2SC{\equiv}C$[g]	**33**	8	5.8×10^5	0.096	0.31	4s
C≡C-*p*-C_6H_4C≡C	**34**	8	2.6×10^4	0.076	0.25	4m,r
$C{\equiv}CC_{14}H_8C{\equiv}C$[h]	**35**	8	1.3×10^6	0.038	0.27	4q

[a] ***Fe*** = FeCp*(dppe). [b] The number of carbon atoms spanning the two Fe centers. [c] Bu_4NPF_6 (electrolyte) in CH_2Cl_2. [d] Estimated as class II compounds (see text).[27] [e] Estimated as class III compounds (see text).[27] [f] Present work. [g] C_4H_2S = thiophene-2,5-diyl. [h] $C_{14}H_8$ = anthracene-9,10-diyl.

The *E* and *Z* isomers of the C_6H_2 complex, (*E*)- and (*Z*)-**11**, are distinguishable by the spectroscopic (NMR and IR) and electrochemical features, and no isomerization is observed, in contrast to the C_8 complex **17** with the diene linker. Taking into account the molecular structure of the C_6 precursor (*Z*)-**16**, the bulky ancillary ligands (Cp* and dppe) may engage with each other to freeze the olefin isomerization. The K_C values for the two isomers are comparable, but the *E* isomer with a longer metal−metal distance shows a slightly larger K_C value.[31]

As far as the C_6 complexes (hex-3-ene-1,5-diyne-1.6-diyl complexes) ***Fe***−C≡C−(R)C=C(R)C≡C−***Fe***, are concerned, a substituent effect (R) is evident: K_C for R = aryl (**27**) > C≡C−R′ (**6**, **7**) > H (**11**). Because no apparent relationship with the σ_p parameter (−0.01 (Ph) ≈ H (0) < 0.23 (C≡C−H))[32] is present, the high performance of the aryl derivatives **27** should be ascribed to the delocalization of the odd electron over the π-system extended to the R groups. In addition, the effect of the CF_3 group in **27b** is notable. The introduction of the CF_3 groups causes substantial shifts of the two redox potentials to the positive side, in accord with the electron-withdrawing nature of the CF_3 group, but the K_C value of **27b** is twice as large as that of the parent compound **27a**, though not significant, in contrast to our expectation that the electron-deficient cation-radical species would be destabilized by an electron-withdrawing group to show a smaller K_C value. Although very few studies on the related substituent effect have appeared, it was reported that introduction of the OMe groups at the 1- and 4-positions of the butadiene-1,4-diyl system (K_C(**29**; OMe)/K_C(**28**; H) = 1.5×10^{-3}) caused a drastic decrease of the K_C values (Table 4).[21d] The large difference has been interpreted in terms of stabilization of the dication by neutralization of the positive charges by the π-electron-donating OMe substituents. In the case of the CF_3 complex **27b**, the electron-withdrawing CF_3 group should destabilize not only the monocation but also the dication. When the shifts caused by the replacement of H by CF_3 are compared, the CF_3 substitution influences the second redox process (Fe(II)−Fe(III) → Fe(III)−Fe(III): −557 mV (**27a**) → −417 mV (**27b**); 140 mV) more significantly than the initial redox process (Fe(II)−Fe(II) → Fe(II)−Fe(III): −1092 mV (**27a**) → −972 mV (**27b**); 120 mV), leading to a larger separation of the two redox processes; i.e., a larger K_C value. The V_{ab}^{III} values show the tendency that we expected (0.40 (**27a**) > 0.39 (**27b**)), although the difference is not significant.

A comparison of the performance of the C≡C and C=C units can be made. As already pointed out by Sponsler[21c] for the C_4 system, the C≡C unit is better than the C=C unit, as can be seen from **28** and **30** (K_C(**28**)/K_C(**30**) = 1.1×10^{-2}). The same tendency is observed for the C_6 system with one C=C unit (K_C-(**11**)/K_C(**31**) = 1.2×10^{-1}) and the C_8 system with two C=C units (K_C(**17**)/K_C(**32**) = 2.4×10^{-3}), and thus, replacement of one C≡C unit in a certain conjugated bridge by the C=C unit would cause an exponential decrease of the K_C value (at least 10^{-1} times smaller by one replacement). The C_8 complex **17** lies between complexes **33** and **34** with the aromatic linker in the central part, where the two iron centers are also separated by eight carbon atoms. The most significant feature of the enyne system is that the performance can be tuned by introducing appropriate substituents on the C=C part. As typically exemplified by the series of C_6 complexes obtained by the present study, introduction of the aryl groups onto the C=C part improves the performance 25 times greater than for the parent complex **11**.

Conclusion

A series of the redox-active diiron complexes consisting of combinations of the C≡C and C=C units has been prepared and characterized by spectroscopic and crystallographic methods. The C_6 hex-3-ene-1,5-diyne-1,6-diyl complexes with substituents at the C3 and C4 carbon atoms show two well-separated, reversible redox waves, suggesting formation of stable monocationic, mixed-valence states upon one-electron oxidation. The comproportionation constants K_C exceed 10^8, leading to the classification to class III compounds according to the Robin and Day classification. All of the diiron complexes obtained by the present study afford isolable mono- and dications upon chemical oxidation with the ferrocenium cation, and the isolated monocations exhibit intense absorptions in the near-IR region, which are ascribed to the intervalence charge transfer (IVCT) band of a highly delocalized π-conjugated system. The V_{ab} values derived from the IVCT bands are so large that the diiron complexes belong to class III Robin−Day compounds. In comparison with a related polyynediyl system consisting only of the C≡C unit, the performance is slightly inferior, but the performance can be tuned by introduction of appropriate substituents onto the olefinic carbon atoms (Scheme 1). The

(31) In the *Z* isomer, the engaging of the bulky Fe fragments may distort the central olefinic part from a planar structure to cause a decrease of the overlap of the π-system or the Fe−C_α orbital interaction.

(32) Johnson, C. D. *The Hammett Equation*; Cambridge University Press: Cambridge, U.K., 1973.

present study suggests that the stability of the monocation may be tuned by delocalization of the radical cation over the attached substituents.

Functionalization of the olefinic part would lead to a sophisticated system. For example, introduction of functional groups responsive to the environment (e.g. pH, heat, and irradiation) would be able to introduce a switching function. Studies targeting such a system as well as higher order systems (Scheme 1) are now under way, and the results will be reported in forthcoming papers.

Experimental Section

General Methods. All manipulations were carried out under an inert atmosphere by using standard Schlenk tube techniques. THF, ether, hexane (Na−K alloy), CH_2Cl_2 (P_2O_5), and ROH ($Mg(OR)_2$; R = Me, Et) were treated with appropriate drying agents, distilled, and stored under argon. ^1H and ^{13}C NMR spectra were recorded on Bruker AC-200 (^1H, 200 MHz; ^{31}P, 81 MHz) and JEOL EX-400 spectrometers (^1H, 400 MHz; ^{13}C, 100 MHz). Chemical shifts (downfield from TMS (^1H and ^{13}C) and H_3PO_4 (^{31}P)) and coupling constants are reported in ppm and in Hz, respectively. Solvents for NMR measurements containing 0.5% TMS were dried over molecular sieves, degassed, distilled under reduced pressure, and stored under Ar. IR and UV−vis−near-IR spectra were obtained on a JASCO FT/IR 5300 spectrometer and a JASCO V-570 spectrometer, respectively. ESI-MS and FD/FAB-MS spectra were recorded on a ThermoQuest Finnigan LCQ Duo mass spectrometer and a JEOL JMS-700 mass spectrometer, respectively. For cationic complexes, M stands for the molecular weight for the cationic fragment. Electrochemical measurements were made with a BAS 100B/W analyzer. ***Fe***−Cl,[33] **3**,[14c] **4**,[15] **8a**,[4c] **8b**,[4f] (*E*)-**12**,[20] (*Z*)-**12**,[20] **18**,[21e] **21**,[21g] **26**,[34] and $FcPF_6$[35] were prepared according to the published procedures. Other chemicals were purchased and used as received.

1:4 Reaction between 3 and *Fe*-Cl (Reaction I): Preparation of 6. A mixture of **3** (165 mg, 0.40 mmol), ***Fe***−Cl (1.00 g, 1.60 mmol), KF (93 mg, 1.6 mmol), and KPF_6 (294 mg, 1.60 mmol) was dissolved in MeOH (130 mL)−THF (13 mL) refluxed for 7 h, upon which it turned purple. Then the volatiles were removed under reduced pressure, and the resultant residue was extracted with ether. The ethereal extract was passed through an alumina plug, and the filtrate was evaporated under reduced pressure. The resultant residue was washed with MeCN at room temperature and then with pentane at −78 °C. The obtained purple powder was dried in vacuo: **6** (399 mg, 0.28 mmol, 69%). UV−vis (in THF): λ_{max}/nm (ϵ_{max}/M^{-1} cm^{-1}) 578 (3.05×10^4), 800 (4.0×10^3). FD-MS: *m*/*z* 1446 (M^+). Anal. Calcd for $C_{88}H_{96}Si_2P_4Fe_2$: C, 73.12; H, 6.69. Found: C, 72.91; H, 6.50.

Preparation of 7. (i) Reactions II and III. A methanolic solution (12 mL) containing **3** (300 mg, 0.728 mmol) and K_2CO_3 (48 mg, 0.35 mmol) was stirred for 30 min and then extracted with pentane (5 mL × 3). The pentane layer containing **5** was washed with water (3 mL × 3), dried over Na_2SO_4, and concentrated to ca. 5 mL under reduced pressure. (*Caution! Because a concentrated sample of compound **5** is explosive, a small amount of pentane should be left.*) ***Fe***−Cl (300 mg, 0.47 mmol) and KPF_6 (89 mg, 0.47 mmol) were weighed into a separate Schlenk tube and dissolved in MeOH (63 mL)−THF (7 mL). To the mixture was added the pentane solution of crude **5**, and the resultant mixture was stirred for 24 h. Then the volatiles were removed under reduced pressure, and THF (20 mL) and KOBu^t (100 mg) were added to the residue. The mixture was stirred for 2 h, and the volatiles were removed under reduced pressure. The product was extracted with ether and passed through an alumina plug. After removal of the volatiles under reduced pressure, the residue was washed with MeCN. Crystallization of the residue from toluene−ether gave **7** as deep purple crystals (263 mg, 0.202 mmol, 28% based on **3**). FD-MS: *m*/*z* 1300 (M^+). Anal. Calcd for $C_{82}H_{80}P_4Fe_2$: C, 75.70; H, 6.20. Found: C, 75.50; H, 6.31.

(ii) Reaction IV. A THF solution (20 mL) containing **6** (194 mg, 0.134 mmol) and Bu_4NF (1 M THF solution, 0.05 mL, 0.05 mmol) was stirred for 2 h. After removal of the volatiles under reduced pressure the residue was washed with pentane at −78 °C and crystallized from THF−pentane to give **7** (143 mg, 0.110 mmol, 82%).

Preparation of (*E*)-11. (i) Reaction VI. A mixture of (*E*)-**12** (150 mg, 0.68 mmol), ***Fe***−Cl (1.019 g, 1.63 mmol), KPF_6 (300 mg, 1.63 mmol), and KF (95 mg, 1.63 mmol) dissolved in MeOH (50 mL)−THF (5 mL) was stirred for 24 h at room temperature. After removal of the volatiles under reduced pressure the residue was washed with pentane. KOBu^t (153 mg, 1.36 mmol) and THF (10 mL) were added to the residue, and the resultant mixture was stirred for 30 min. The product was extracted with ether and passed through an alumina column. After removal of the volatiles under reduced pressure the residue was washed with MeCN. Crystallization of the residue from ether−pentane gave (*E*)-**11** as a red powder (8 mg, 0.064 mmol, 1%). (*E*)-**11**: FD-MS *m*/*z* 1252 (M^+).[36a]

(ii) Reactions VII and VIII. A mixture of (*E*)-**12** (106 mg, 0.58 mmol), ***Fe***−Cl (300 mg, 0.58 mmol), KPF_6 (107 mg, 0.58 mmol), and KF (34 mg, 0.58 mmol) dissolved in MeOH (50 mL)−THF (5 mL) was stirred for 6 h at room temperature. The product was extracted with ether and passed through an alumina column. After removal of the volatiles under reduced pressure, the residue was extracted with MeCN, and cooling to −30 °C gave (*E*)-**13** as orange crystals (147 mg, 0.20 mmol, 34%). (*E*)-**13**: δ_H (C_6D_6) 6.66 (dt, J = 15.6, 2.3, Fe−C≡C−CH═), 5.73 (d, J = 15.6, ═CHC≡C−$SiMe_3$), 1.43 (s, Cp*), 0.24 (s, $SiMe_3$); δ_P (C_6D_6) 92.6; δ_C (C_6D_6) 155.9 (t, J_{CP} = 40, C_α), 129.0 (s, C≡C), 121.8 (d, J_{CP} = 6, C≡C), 108.9 (d, J_{CP} = 9, C≡C), 108.7 (d, J_{CH} = 163, ═CH), 94.4 (s, C≡C), 88.2 (s, C_5Me_5), 31.0 (m, PCH_2), 10.4 (q, J = 126, C_5Me_5), 0.4 (q, J = 119, $SiMe_3$); IR (KBr) 2113, 2016 cm^{-1}; FD-MS 736 (M^+). Anal. Calcd for $C_{45}H_{50}SiP_2Fe_2$: C, 73.36; H, 6.84. Found: C, 73.55; H, 7.12. Repeated metalation of (*E*)-**13** gave a trace amount of (*E*)-**11**.

Preparation of (*Z*)-11. (i) (*Z*)-16 (Reactions XI and XII). A THF solution (5 mL) of (*Z*)-**12** (560 mg, 2.55 mmol) was slowly added to Bu_4NF (1.0 M THF solution 5 mL, 5.0 mmol) dissolved in ethylene glycol (4 mL), and the mixture was stirred for 3 h at room temperature. Most of the THF was removed by a rotary evaporator at room temperature, and the desilylated (*Z*)-**14** was collected in a trap immersed in a liquid N_2 bath by vacuum distillation. To the distillate was added THF (5 mL) at −78 °C. The THF solution of (*Z*)-**14** was slowly added to a mixture of ***Fe***−Cl (1.03 g, 1.65 mmol) and KPF_6 (334 mg, 1.7 mmol) suspended in MeOH (50 mL)−THF (5 mL), and the resultant mixture was stirred for 1 day at room temperature to give a gray-green solution. Then the volatiles were removed under reduced pressure, the residue was extracted with CH_2Cl_2, and the extract was passed through a Celite plug. The volume of the solution was reduced under vacuum, and (*Z*)-**16** was obtained as deep green crystals (1.01 g, 0.65 mmol, 79%) after crystallization from CH_2Cl_2−THF−pentane. (*Z*)-**16**: δ_C ($CDCl_3$) 368.2 (t, J = 35, Fe═C), 134−128 (Ph), 120.2 (d, J = 154, ═CH), 107.1 (d, J = 159, ═CH), 100.8 (C_5Me_5), 29.5 (m,

(33) Roger, C.; Hamon, P.; Toupet, L.; Rabaa, L. Saillard, J.-Y.; Hamon, J.-R.; Lapinte, C. *Organometallics* **1991**, *10*, 1045.

(34) Jones, G. B.; Wright, J. M.; Hynd, G.; Huber, R. S.; Mathews, J. E. *J. Am. Chem. Soc.* **2000**, *122*, 1937.

(35) Gray, H. B.; Hendrickson, D. N.; Sohn, Y. S. *Inorg. Chem.* **1971**, *10*, 1559. Duggan, D. M.; Henrickson, D. N. *Inorg. Chem.* **1975**, *14*, 955.

(36) (a) Elemental analysis could not be performed due to the low yield. (b) Undesired products were characterized only by spectroscopy and crystallography. (c) An analytically pure sample could not be obtained, despite several attempts.

PCH_2), 10.1 (q, $J = 126$, C_5Me_5). Anal. Calcd for $C_{81}H_{88}F_{12}P_6Cl_6Fe_2$ (**16**·$3CH_2Cl_2$): C, 54.14; H, 4.94. Found: C, 54.05; H, 4.93.

(ii) (*Z*)-11 (Reactions XI−XIII: without Isolation of (*Z*)-16). A solution of (*Z*)-**16** was generated by starting from (*Z*)-**12** (560 mg, 2.55 mmol) as described above. The obtained gray-green solution was evaporated to dryness under reduced pressure, and the residue was washed with pentane (50 mL). Then the obtained residue was treated with $KOBu^t$ (185 mg, 1.65 mmol) in THF (50 mL) for 30 min to give a dark red solution. After the volatiles were removed under reduced pressure, the products were extracted with ether and passed through an alumina plug. Concentration and crystallization from ether−pentane at −30 °C gave (*Z*)-**11** as deep red crystals (750 mg, 0.60 mmol, 73%). (*Z*)-**11**: δ_C (C_6D_6) 139.4 (t, $J = 38$, Fe−C), 141−126 (Ph), 122.5 (s, Fe−C≡*C*), 112.8 (d, $J = 154$, ═CH), 87.9 (C_5Me_5), 31.2 (m, PCH_2), 10.4 (C_5Me_5); UV−vis (in THF) $\epsilon_{max}/M^{-1}cm^{-1}$ (λ_{max}/nm) 404 (5.7×10^3); FD-MS *m*/*z* 1252 (M^+). Anal. Calcd for $C_{76}H_{80}P_4Fe_2$: C, 74.27; H, 6.56. Found: C, 74.52; H, 6.80.

Preparation of (*E,E*)-17: (i) Reaction XIV. A mixture of **18** (70 mg, 0.29 mmol), ***Fe***−Cl (358 mg, 0.58 mmol), KPF_6 (105 mg, 0.57 mmol), and KF (40 mg, 0.69 mmol) dissolved in MeOH (50 mL)−THF (5 mL) was refluxed for 8 h. After removal of the volatiles, the residue was washed with ether and extracted with THF. The THF extract was passed through an alumina plug, and the residue obtained by removal of the volatiles under reduced pressure was washed with MeCN and crystallized from THF−ether to give (*E,E*)-**17** as red-orange crystals (105 mg, 0.082 mmol, 28% based on **18**). (*E,E*)-**17**: UV−vis (in THF) λ_{max}/nm (ϵ_{max}/M^{-1} cm^{-1}) 452 (1.6×10^4); FD-MS *m*/*z* 1278 (M^+). Anal. Calcd for $C_{98}H_{100}P_4Fe_2$ (**17**·3(benzene): C, 77.77; H, 6.66. Found: C, 77.36; H, 6.72.

(ii) Reactions XV−XVII. To an ethanolic solution (3 mL) of **19** (50 mg, 0.20 mmol) were added water (0.36 mL) and 50% NaOH solution (0.36 mL), and the resultant mixture was stirred for 3 h. Then the desilylated **18** was extracted with pentane, and the extract was evaporated under reduced pressure and dissolved in THF. (*Caution! Because a concentrated sample of compound **19** may be explosive, a small amount of pentane should be left.)* ***Fe***−Cl (152 mg, 0.24 mmol) and KPF_6 (45 mg, 0.24 mmol) were weighed into a separate Schlenk tube and dissolved in MeOH (20 mL)−THF (2 mL). To the mixture was added the crude THF solution of **19**, and the resultant mixture was stirred for 24 h. Then the volatiles were removed under reduced pressure. The residue was washed with ether and crystallized from MeCN−ether, giving (*E,E*)-**17** as dark yellow-green crystals (44 mg, 0.028 mmol, 14% based on **18**). (*E,E*)-**17**: δ_C (CD_3CN) 367.2 (t, $J_{CP} = 33$, Fe═C), 134−128 (Ph), 125.0 (d, $J_{CH} = 152$, ═CH), 124.3 (d, $J_{CH} = 152$, ═CH), 116.3 (d, $J_{CH} = 148$, ═CH), 101.1 (C_5Me_5), 29.8 (m, PCH_2), 10.2 (q, $J_{CH} = 127$, C_5Me_5); ESI-MS *m*/*z* 1424 ($M^+ - H + PF_6$), 640 (M^{2+}). To a THF solution of **20** (29 mg, 0.023 mmol) was added $KOBu^t$ (10 mg, 0.1 mmol), and the mixture was stirred for 30 min. Then the volatiles were removed under reduced pressure, and the resultant residue was extracted with benzene and crystallized from benzene−ether, giving (*E,E*)-**17** (23 mg, 0.018 mmol, 78%).

Preparation of 21. $Me_3SiC{\equiv}C{-}C{\equiv}CH$[37] (323 mg, 2.65 mmol), **23b** (*E,Z* mixture, 0.10 mL, 1.26 mmol), $Pd(PPh_3)_4$ (146 mg, 0.21 mmol), and CuI (26 mg, 0.14 mmol) dissolved in degassed NEt_3 (20 mL) were stirred for 16 h at room temperature. After removal of the volatiles under reduced pressure the products were extracted with pentane and separated by silica gel chromatography to give (*E*)-**21** (196 mg, 0.71 mmol, 56%) and (*Z*)-**21** (95 mg, 0.34 mmol, 27%) as yellow oils. (*E*)-**21**: δ_H ($CDCl_3$) 6.11 (2H, s, ═CH), 0.21 (18H, s, $SiMe_3$); δ_C ($CDCl_3$) 123.0 (d, $J = 170$, ═CH), 94.9, 87.4, 81.4, 74.7 (C≡), −0.3 (q, $J = 128$, Me); IR (KBr) 2201, 2097 cm^{-1}; FAB-MS *m*/*z* 268 (M^+). (*Z*)-**21**: δ_H ($CDCl_3$) 5.96 (2H, s, ═CH), 0.23 (18H, s, $SiMe_3$); δ_C ($CDCl_3$) 121.5 (d, $J = 171$, ═CH), 95.0, 87.7, 83.0, 73.8 (C≡), −0.2 (q, $J = 128$, Me); IR (KBr) 2198, 2181, 2098 cm^{-1}; FAB-MS *m*/*z* 268 (M^+).

Desilylation of (*E*)- and (*Z*)-21. To a stirred ethylene glycol (0.5 mL)−THF (2.5 mL) solution containing Bu_4NF (1 M THF solution, 0.9 mL, 0.9 mmol) was added (*E*)-**21** (113 mg, 0.42 mmol) dropwise, and the resultant mixture was stirred for 3 h at room temperature and then vacuum-transferred to another flask cooled at −78 °C. Most of the volatiles were removed with a water aspirator to leave the desilylated product as oil contaminated with THF and $HOCH_2CH_2OH$. Because the product might be explosive, concentration was stopped and the product was analyzed by NMR. The *Z* isomer can also be generated in essentially the same manner. (*E*)-HC≡C−C≡C−CH═CHC≡C−C≡CH: δ_H ($CDCl_3$) 6.13 (2H, s, ═CH), 2.64 (2H, ≡CH); δ_C ($CDCl_3$) 123.2 (d, $J = 162$, ═CH), 74.8 (d, $J = 257$, ≡CH), 73.0, 67.8, 63.7 (s × 3, C≡C). *Z* isomer: δ_H ($CDCl_3$) 5.98 (s, ═CH), 2.67 (s, ≡CH); δ_C 121.9 (d, $J = 171$, ═CH), 75.0 (d, $J = 261$, CH), 72.2, 68.0, 63.7 (s × 3, C≡C).

Preparation of 24. 24a. To a mixture of **8** (500 mg, 0.81 mmol), $PdCl_2(PPh_3)_2$ (58 mg, 0.082 mmol), CuI (33 mg, 0.17 mmol), and (*E*)-**23a** (X = Cl; 0.63 mL, 8.1 mmol) was added degassed $NHPr^i_2$ (25 mL), and the mixture was refluxed for 8 h. After consumption of **8** was checked by TLC, the volatiles were removed under reduced pressure, the residue was extracted with toluene, and the extract was filtered. After removal of the volatiles the residue was extracted with ether and passed through an alumina pad. Evaporation gave a red oily product, which was triturated with pentane at −78 °C to give **24a** as a red powder (201 mg, 0.30 mmol, 37%). **24a**: δ_H (C_6D_6) 6.36 (dt, $J = 14.0$, 2.0, ≡CCH═), 6.03 ($J = 14.0$, ═CHCl); δ_P (C_6D_6) 92.8; δ_C (C_6D_6) 145.4 (t, $J = 35$, Fe−C≡), 128−140 (Ph), 120.2 (d, $J = 153$, C═C), 119.1 (d, $J = 189$, C═C), 115.0 (s, Fe−C≡*C*), 87.9 (s, C_5Me_5), 31.0 (t, $J = 22$, PCH_2), 10.4 (q, $J = 123$, C_5Me_5); IR (KBr) 2027 cm^{-1}.[36b]

24b. To a mixture of **8** (300 mg, 0.48 mmol), $PdCl_2(PPh_3)_2$ (35 mg, 0.049 mmol), and CuI (20 mg, 0.10 mmol) were added THF (2 mL), **23b** (*E* and *Z* mixture; 0.82 mL, 0.96 mmol), and degassed NEt_3 (5 mL), and the mixture was stirred for 40 h at room temperature. After consumption of **8** was checked by TLC, the volatiles were removed under reduced pressure, the residue was extracted with ether, and the extract was passed through an alumina plug. After removal of the volatiles the residue was extracted with pentane. The red oily residue obtained by evaporation was triturated with pentane at −78 °C to give **24b** as a red powder (76.0 mg, 0.11 mmol, 22%). **24b** (a 2:1 mixture of *E* and *Z* isomers): *m*/*z* 1180 (M^+). *E* isomer: δ_H (C_6D_6) 6.59 (dt, $J = 13.3$, 2.1, ≡CCH═), 6.08 (d, $J = 13.3$, ═CHBr), 1.44 (s, Cp*); δ_P (C_6D_6) 92.7. *Z* isomer: δ_H (C_6D_6) 6.42 (dt, $J = 6.6$, 2.0, ≡C−CH═), 5.59 (d, $J = 6.6$, ═CHBr), 1.52 (s, Cp*). δ_P (C_6D_6) 93.1.

Reaction between 24b and 8. Reaction among **24b** (83 mg, 0.115 mmol), **8** (71 mg, 0.115 mmol), $Pd(PPh_3)_4$ (8.3 mg, 0.0012 mmol), and CuI (4 mg, 0.02 mmol) in NEt_3 for 45 h at room temperature followed by workup as described for **24b** gave a mixture of **25** and **10b**, as revealed by ^1H NMR. **25**: δ_H (C_6D_6) 6.20 (ddt, $J = 17.0$, 10.4, 2.2, ≡CCH═), 5.22 (dd, $J = 17.0$, 3.3, CH_2), 4.93 (dd, $J = 10.4$, 3.3, ═CH_2), 1.44 (s, Cp*); δ_P (C_6D_6) 93.5. Complex **10b** was identified by comparison with an authentic sample.[4b,c]

Preparation of 27 (Reaction XIX). As a typical example, the preparative procedures for **27a** are described. To a THF solution (5 mL) of **26a** (244 mg, 0.45 mmol) cooled in a dry ice−acetone bath was added Bu_4NF (1 M THF solution, 1 mL, 1.0 mmol), and the mixture was stirred for 30 min. Then water was poured into the mixture and the product was extracted with pentane. The pentane layer was separated, and the solvent was removed under reduced pressure. To the residue were added THF (15 mL)−MeOH (1.5 mL), ***Fe***−Cl (353 mg, 0.56 mmol), and KPF_6 (119 mg, 0.65 mmol) under argon, and the mixture was stirred for 31 h. After removal of the volatiles the residue was washed with toluene. Then $KOBu^t$

(37) Bartik, B.; Dembinski, R.; Bartik, T.; Arif, A. M.; Gladysz, J. A. *New J. Chem.* **1997**, *21*, 739.

Table 5. Crystallographic Data

	6·6CH_2Cl_2	**7**	**10a**·2Et_2O	**13**	**15**·2MeCN
formula	$C_{94}H_{108}Si_2P_4Cl_{12}Fe_2$	$C_{82}H_{80}P_4Fe_2$	$C_{88}H_{98}O_2P_4Fe_2$	$C_{45}H_{50}SiP_2Fe$	$C_{46}H_{50}N_2P_2Fe$
formula wt	1955.08	1301.12	1423.33	736.77	748.71
cryst syst	triclinic	monoclinic	triclinic	monoclinic	monoclinic
space group	$P\bar{1}$	$P2_1/c$	$P\bar{1}$	$C2/c$	$P2_1/n$
a/Å	15.247(1)	17.4725(9)	10.919(8)	47.2573(8)	20.80(1)
b/Å	15.708(2)	11.0643(4)	12.218(10)	18.2182(3)	10.369(7)
c/Å	12.407(2)	17.9715(9)	15.67(1)	20.4735(3)	20.79(1)
α/deg	111.850(1)	90	72.04(3)	90	90
β/deg	105.193(4)	106.615(3)	79.77(3)	102.0703(9)	115.02(2)
γ/deg	62.000(7)	90	87.96(3)	90	90
V/Å^3	2421.3(5)	3329.2(3)	1956(2)	17236.8(5)	4062(4)
Z	1	2	1	16	4
d_{calcd}/g cm^{-3}	1.341	1.298	1.208	1.136	1.224
μ/mm^{-1}	0.668	0.577	0.498	0.479	0.483
no. of diffractions collected	17 456	27 107	14 859	68 068	25 365
no. of variables	515	410	433	895	460
R1 for data with $I > 2\sigma(I)$	0.0783 (for 6596 data)	0.0461 (for 6093 data)	0.0603 (for 3791 data)	0.0587 (for 9097 data)	0.0540 (for 3217 data)
wR2	0.2105 (for all 9894 data)	0.1379 (for all 7490 data)	0.1778 (for all 8090 data)	0.1733 (for all 19 024 data)	0.1765 (for all 8436 data)

	16·4CH_2Cl_2	**17**·3C_6H_6	**20**·6MeCN	**6**$^+PF_6^-$·MeCN
formula	$C_{82}H_{90}F_{12}P_6Cl_8Fe_2$	$C_{98}H_{100}P_4Fe_2$	$C_{92}H_{102}N_6F_{12}P_6Fe_2$	$C_{90}H_{99}NF_6Si_2P_5Fe_2$
formula wt	1884.75	1513.46	1817.38	1631.50
cryst syst	triclinic	monoclinic	monoclinic	rhombohedral
space group	$P\bar{1}$	$P2_1/n$	$P2_1/c$	$R\bar{3}$
a/Å	11.107(2)	14.977(8)	12.932(4)	19.06(1)
b/Å	11.477(3)	12.689(9)	20.910(6)	19.06(1)
c/Å	18.169(4)	22.77(2)	17.410(3)	19.06(1)
α/deg	102.282(7)	90	90	91.07(1)
β/deg	103.041(12)	108.30(3)	108.19(1)	91.07(1)
γ/deg	100.894(10)	90	90	91.07(1)
V/Å^3	2135.3(8)	4108(4)	4472(2)	6918(6)
Z	1	2	2	3
d_{calcd}/g cm^{-3}	1.466	1.223	1.349	1.175
μ/mm^{-1}	0.771	0.477	0.505	0.480
no. of diffractions collected	17 294	26 162	34 841	44 961
no. of variables	507	478	535	497
R1 for data with $I > 2\sigma(I)$	0.0632 (for 6014 data)	0.0637 (for 3008 data)	0.0808 (for 5101 data)	0.0797 (for 6025 data)
wR2	0.1773 (for all 8893 data)	0.2002 (for all 8875 data)	0.2179 (for all 9449 data)	0.2400 (for all 10 529 data)

(150 mg, 1.33 mmol) and THF (15 mL) were added, and the mixture was stirred for 30 min. Removal of the volatiles, extraction with toluene, filtration through an alumina plug, and precipitation from toluene−MeCN gave **27a** (180 mg, 0.13 mmol, 28%) as a red powder. **27a**: UV−vis (in THF) λ_{max}/nm (ϵ_{max}/M^{-1} cm^{-1}) 452 (2.1×10^4); FD-MS m/z 1405 (M^+). Anal. Calcd for $C_{90}H_{88}P_4Fe_2$: C, 76.92; H, 6.31. Found: C, 77.07; H, 6.18. **27b**: UV−vis (in THF) λ_{max}/nm (ϵ_{max}/M^{-1} cm^{-1}) 222 (6.5×10^4), 506 (1.3×10^4); FD-MS m/z 1540 (M^+).[36c]

Electrochemical Measurements. CV and DPV measurements were performed with a Pt electrode for CH_2Cl_2 solutions of the samples (~2×10^{-3} M) in the presence of an electrolyte (Bu_4NPF_6: 0.1 M) at room temperature under an inert atmosphere. The scan rates were 100 mV/s (CV) and 20 mV/s (DPV). After the measurements, ferrocene (Fc) was added to the mixture and the potentials were calibrated with respect to the Fc/Fc^+ redox couple.

Preparation of Mono- and Dicationic Species. As typical examples, procedures for the cationic species derived from **6** are described. Most of the mono- and dications were characterized spectroscopically.

(i) Preparation of 6$^+PF_6^-$. A mixture of **6** (50.0 mg, 0.035 mmol) and $FcPF_6$ (8.2 mg, 0.025 mmol) was stirred for 3 h at room temperature. After removal of the volatiles under reduced pressure the residue was washed with ether and recrystallized from CH_2Cl_2−ether, giving **6**$^+PF_6^-$ (37 mg, 0.023 mmol, 93%) as deep green crystals.

(ii) Preparation of 6^{2+}(PF_6^-)$_2$. Reaction of **6** with 1.9 equiv of $[FeCp_2]PF_6$ gave **6**$^{2+}$(PF_6^-)$_2$ as deep blue crystals.

6$^+PF_6^-$: UV−vis (in CH_3CN) λ_{max}/nm (ϵ_{max}/M^{-1}·cm^{-1}) 798 (2.5×10^4), 1692 (1.3×10^4). Anal. Calcd for $C_{88}H_{96}F_6Si_2P_5Fe_2$: C, 66.46; H, 6.08. Found: C, 66.14; H, 6.14. **6**$^{2+}$(PF_6^-)$_2$: IR, no characteristic band; UV−vis (in CH_3CN) λ_{max}/nm (ϵ_{max}/M^{-1} cm^{-1}) 264 (1.5×10^4), 432 (4.5×10^3), 672 (2.8×10^3). **7**$^+PF_6^-$: Anal. Calcd for $C_{82}H_{80}F_6P_5Fe_2$: C, 68.11; H, 5.50. Found: C, 67.88; H, 5.21. (*Z*)-**11**$^+PF_6^-$: UV−vis (in CH_3CN) λ_{max}/nm (ϵ_{max}/M^{-1} cm^{-1}): 404 (5.0×10^3), 628 (1.5×10^4), 1586 (1.6×10^4). (*Z*)-**11**$^{2+}$-(PF_6^-)$_2$: δ_H (CD_2Cl_2) 8.08 (2H, m, ═CH), 7.60−6.70 (Ph), 4.15, 3.13 (2H × 2, CH_2P), 1.30 (30H, s, Cp*); δ_P (CD_2Cl_2) 75.2; IR, no characteristic band; UV−vis (in CH^3CN) λ_{max}/nm (ϵ_{max}/M^{-1} cm^{-1}) 270 (7.6×10^3), 400 (1.5×10^3), 646 (1.3×10^4). (*E*,*E*)-**17**$^+PF_6^-$: UV−vis (in CH_3CN) λ_{max}/nm (ϵ_{max}/M^{-1}·cm^{-1}) 266 (3.1×10^4), 452 (8.3×10^3), 682 (3.9×10^4), 1930 (5.7×10^3); ESI-MS m/z 1278 ($M^+ + PF_6$). (*E*,*E*)-**17**$^{2+}$(PF_6^-)$_2$: δ_H (CD_3CN) 8.74 (2H, m, ═CH), 7.55−6.82 (Ph), 6.54 (2H, m, ═CH), 3.80, 2.95 (2H × 2, CH_2P), 1.28 (30H, s, Cp*); δ_P (CD_3CN) 78.2; IR 1905 cm^{-1}; UV−vis (in CH_3CN) λ_{max}/nm (ϵ_{max}/M^{-1} cm^{-1}) 266 (3.1×10^4), 452 (8.3×10^3), 682 (3.9×10^4), 1930 (5.7×10^3); ESI-MS m/z 1423 ($M^+ + PF_6$), 639 (M^{2+}). **27a**$^+PF_6^-$: UV−vis (in CH_3CN) λ_{max}/nm (ϵ_{max}/M^{-1} cm^{-1}) 406 (9.7×10^3), 636 (1.9×10^4), 1556 (2.2×10^4); FD-MS 1423 ($M^+ + PF_6$), 639 (M^{2+}). **27a**$^{2+}$-(PF_6^-)$_2$: δ_H (CD_3CN) 7.71−6.35 (Ph), 2.90−2.46 (2H × 2, CH_2P), 1.03 (30H, s, Cp*); δ_P (CD_3CN) 82.6; IR 1630 cm^{-1}; UV−vis (in

CH_3CN) λ_{max}/nm (ϵ_{max}/M^{-1} cm^{-1}) 270 (2.6×10^4), 384 (3.4×10^3), 668 (1.6×10^4); ESI-MS *m*/*z* 1549 ($M^+ + PF_6$), 1404 (M^+). **27b**$^+PF_6^-$: UV−vis (in CH_3CN) λ_{max}/nm (ϵ_{max}/M^{-1} cm^{-1}): 392 (1.6×10^4), 654 (2.1×10^4), 1596 (1.9×10^4); FD-MS *m*/*z* 1686 ($M^+ + PF_6$), 1540 (M^+). **27b**$^{2+}(PF_6^-)_2$: δ_H (CD_3CN) 7.76−6.63 (Ph), 3.05, 2.68 (2H × 2, CH_2P), 0.99 (30H, s, Cp*); δ_P (CD_3CN) 80.9; IR 1614 cm^{-1}; UV−vis (in CH_3CN) λ_{max}/nm (ϵ_{max}/M^{-1} cm^{-1}) 268 (4.0×10^4), 410 (6.7×10^3), 654 (4.3×10^4); FD-MS *m*/*z* 1686 ($M^+ + PF_6$), 1540 (M^+).

X-ray Crystallography. Diffraction measurements were made on a Rigaku RAXIS IV imaging plate area detector with Mo Kα radiation (λ = 0.710 69 Å) at −60 °C. Indexing was performed from 3 oscillation images, which were exposed for 3 min. The crystal-to-detector distance was 110 mm ($2\theta_{max}$ = 55°). In the reduction of data, Lorentz and polarization corrections and empirical absorption corrections were made.[38] Crystallographic data and results of structure refinements are given in Table 5.

The structural analysis was performed on an IRIS O2 computer using the teXsan structure solving program system obtained from the Rigaku Corp., Tokyo, Japan.[39] Neutral scattering factors were obtained from the standard source.[40]

The structures were solved by a combination of direct methods (SHELXS-86)[41] and Fourier synthesis (DIRDIF94).[42] Least-squares refinements were carried out using SHELXL-97[41] (refined on F^2) linked to teXsan. Unless otherwise stated, all non-hydrogen atoms were refined anisotropically; methyl hydrogen atoms were refined using riding models and fixed at the final stage of the refinement, and other hydrogen atoms were fixed at the calculated positions. Structural data for **10a**, **13**, and **15** are included in the Supporting Information.

6: The molecule sat on a crystallographic inversion center. The C1 atom and one of the CH_2Cl_2 solvate molecules were found to be disordered. The C1 atom was refined anisotropically, taking into account two components (C1:C1A = 0.55:0.45). The CH_2Cl_2 solvate molecule was refined isotropically, taking into account two components (Cl5−C73−Cl6:Cl5a−C73a-Cl6a = 0.65:0.35), and the hydrogen atoms attached to the disordered solvate molecule were not included in the refinement.

7: The molecule sat on a crystallographic inversion center. The disordered central part was refined, taking into account two components (C1,2,3,5:C1A,2A,3A,5A = 0.76:0.24).

10a: The molecule sat on a crystallographic inversion center.

13: A unit cell contained two independent molecules, one of which was found to be disordered and refined, taking into account two components (C4B−C5B−C6B:C4C−C5C−C6C = 0.64:0.36). The C4C, C5C, and C6C atoms were refined isotropically, and hydrogen atoms attached to the disordered part were not included in the refinement.

16: The molecule sat on a crystallographic inversion center. The disordered central part was refined, taking into account two components (C3−H2−H3:C3A−H2A−H3A = 1:1). One of the CH_2Cl_2 solvate molecules was also found to be disordered and was refined isotropically, taking into account two components (Cl3−C71−Cl4:Cl3A−C71A-Cl4A = 0.58:0.42), and hydrogen atoms attached to the disordered part were not included in the refinement.

17: The molecule sat on a crystallographic inversion center. The disordered central part was refined, taking into account two components (C4:C4A = 0.658:0.342), and hydrogen atoms attached to the disordered part were not included in the refinement.

20: The molecule sat on a crystallographic inversion center.

6$^+PF_6^-$: The molecule sat on a crystallographic inversion center and was found to be disordered. The olefinic part (C3−C3*:C3A−C3A* = 0.76:0.24) and a part of the $Me_3SiC{\equiv}C$ part (C4,5,7,8-Si1:C4B,5B,7B,8B,Si1B = 0.58:0.42) disordered independently were refined anisotropically, taking into account minor components. The MeCN solvate molecule was refined isotropically. Hydrogen atoms attached to the disordered parts and the solvate molecule were not included in the refinement. The PF_6 anions sat on two 6-fold inversion sites, and only two-thirds of the anions could be located. This should be a result of disorder of the anion, and the other disordered anion could not be located. Another possible interpretation is that the crystal consists of a 2:1 disordered mixture of **6**$^+PF_6^-$ and **6**. Because, however, the single crystals did not show the $\nu_{C{\equiv}C}$ vibration for **6**, the latter possibility has been eliminated.

Acknowledgment. We are grateful to Dr. Toshiro Takao (Tokyo Institute of Technology) for his help for the ^1H NMR simulation. This research was financially supported by the Ministry of Education, Culture, Sports, Science and Technology of the Japanese Government (Grant-in-Aid for Scientific Research on Priority Areas, No. 18065009) and the Japan Society for Promotion of Science and Technology (Grant-in-Aid for Scientific Research (B), No. 15350032), which are gratefully acknowledged.

Supporting Information Available: Tables, figures, and CIF files giving crystallographic results. This material is available free of charge via the Internet at http://pubs.acs.org.

OM060403T

(38) Higashi, T. Program for Absorption Correction; Rigaku Corp., Tokyo, Japan, 1995.

(39) teXsan: Crystal Structure Analysis Package, version 1.11; Rigaku Corp., Tokyo, Japan, 2000.

(40) *International Tables for X-ray Crystallography*; Kynoch Press: Birmingham, U.K., 1975; Vol. 4.

(41) (a) Sheldrick, G. M. SHELXS-86: Program for Crystal Structure Determination; University of Göttingen, Göttingen, Germany, 1986. (b) Sheldrick, G. M. SHELXL-97: Program for Crystal Structure Refinement; University of Göttingen, Göttingen, Germany, 1997.

(42) Beurskens, P. T.; Admiraal, G.; Beurskens, G.; Bosman, W. P.; Garcia-Granda, S.; Gould, R. O.; Smits, J. M. M.; Smykalla, C. The DIRDIF Program System; Technical Report of the Crystallography Laboratory; University of Nijmegen, Nijmegen, The Netherlands, 1992.